Presented at The Intern. School of Subnuclear Physics, Erice, 1974

COMITATO NAZIONALE PER L'ENERGIA NUCLEARE
Laboratori Nazionali di Frascati

LNF-74/59(P)
5 Novembre 1974

M. Greco: DEEP INELASTIC PROCESSES FROM A NON-ORTHODOX POINT OF VIEW.

Servizio Documentazione
dei Laboratori Nazionali di Frascati del CNEN
Casella Postale 70 - Frascati (Roma)

DEEP INELASTIC PROCESSES FROM A NON-ORTHODOX POINT OF VIEW

M. Greco

Laboratori Nazionali di Frascati del CNEN, Frascati Italy

(Lectures presented at International School of Subnuclear Physics, Erice, Sicily, July 1974).

1. INTRODUCTION

The simplest picture suggested by the observed scaling behaviour of the structure functions in deep inelastic scattering of leptons off nucleons is that in which hadrons are composed of point constituents or partons[1,2]. With the further identification of the partons with quarks (and antiquarks) one has a simple representation of the quark. light-cone algebra which leads one to deduce[3] a certain number of selection rules, inequalities and sum rules among different structure functions for electro-and neutrino-production. This theoretical framework is quite successful in accounting for the experimental data, with the possible exceptions of the recent results from CEA and SPEAR on e^+e^- annihilation into hadrons[4] x).

On the other hand parton models do not provide enough constraints on the actual magnitude and the explicit ω dependence of the structure functions and we are left with a complete arbitrariness of the parton distribution functions inside the nucleon, which have to be suitably chosen in order to fit the data. Furthermore most of the inequalities and sum rules of the quark parton model can be reproduced[5] by imposing hadron-like duality arguments on the structure functions without having to deal explicitly with quarks as partons. Finally, since in parton models we have to face the problem of why the quarks do not show up in the final state, the question arises naturally as to whether we really need point like quarks to understand deep inelastic phenomena.

In these lectures I would like to discuss deep inelastic processes, from an "unconventional" point of view. It is unconventional in the sense that no elementary constituents are invoked but rather, scaling properties are accomodated in a fairly natural way by imposing on the current-induced processes the regularities we observe in purely hadronic reactions.

The starting point of our non-conventional approach to scaling phenomena, has been the attempt[6-9] to unify the electromagnetic properties of hadrons both in the small $q^2 (q^2 \simeq 0)$ region, where the photon shows an hadron-like behaviour with strong

---

x) Very recent results on single electron (or muon) production in hadronic collision at large transverse momentum, as well as the results the BNL-Columbia experiment on μ-pair production in proton-uranium collisions, also seem to be in disagreement with the quark-parton model predictions. (See for more details the end of section 5.1).

similarities to ordinary strong processes, and large q^2(q^2 both positive and negative) deep inelastic region, where point-like behaviour seems to be suggested. The central idea, borrowed from the dual models, is that the photon is coupled to a Veneziano-like spectrum of vector states whose properties can be deduced by linking consistently various processes corresponding to different q^2 regions.

This scheme, which makes an extensive use of concepts typical of hadron physics, as duality, Regge behaviour, exchange degeneracy, etc., leads to a unified description of many high energy processes involving real, spacelike and time-like photons, with a large degree of predictive power and in very good agreement with experiments[8]. Furthermore this picture can be easily extended[10] to deep inelastic neutrino reactions, providing essentially the same results which have been considered as a big success of the quark-parton model, without having to deal explicity with quarks as partons.

An important and appealing feature which emerges in this approach is that the scaling properties of the structure functions, and the consequent point-like behaviour of the cross sections follow from common properties of scaling shared by strong, electromagnetic and weak interactions.

We will first study e^+e^- annihilation into hadrons, one of the most exiting processes recently explored experimentally, and source of much theoretical embarrassement in these days. The total cross section and single inclusive distributions will be discussed in detail at the light of different sum rules, in strict connection with the experimental data.

Photo- an electroproduction will then be discussed in the framework of two-component duality, with special emphasis on the links which relate these two processes, in the sense that the nucleon structure functions are explicitly and successfully predicted in terms of photoproduction data. The shadowing effect in photon-nuclei collisions (for $q^2 \leq 0$), which has also been a source of embarrassement for many people, will also be discussed along the same lines.

These results are then extended to deep inelastic neutrino reactions, providing further relations among many different reactions and consistency with the quark parton model results. As a general feature in fact, all our scaling results coincide with those of the parton model so far as the integrated cross sections are concerned.

This consistent picture is completed by considering inclusive processes as $pp \to \mu^+ \mu^- +$ anything and $\gamma(q^2) + p \to h +$ anything in the photon fragmentation region, where a predicted increase with Q^2 of the average transverse momentum of the lepton pair and produced hadrons respectively, is the main departure from conventional parton models.

2. e^+e^- ANNIHILATION INTO HADRONS

2.1. The extended vector-dominance model.

One starts[8] by assuming an infinite number of vector mesons with a linear mass spectrum inspired by dual models

$$m_n^2 = m_o^2 (1 + an), \qquad n = 0, 1, 2, \ldots\ldots \tag{2.1}$$

where a is a constant, which will be determined from photoproduction to be equal to two. One therefore has a pure Veneziano-like spectrum and therefore vector mesons at m_ϱ = = 770 MeV, $\sqrt{3}\, m_\varrho \simeq$ 1300 MeV, $\sqrt{5}\, m_\varrho$ = 1700 MeV, and so forth, and similarly for the isoscalar states. The isovector state at $\sim \sqrt{5}\, m_\varrho$ can be identified with the $\varrho'(1600)$ recently observed at Frascati[11] and SLAC[12] with $\Gamma_\varrho \sim .35$ GeV, $\varrho\pi\pi$ as the main decay mode and $(f_{\varrho'}/f_\varrho)^2 \approx$ 4-5. We have defined $e\, m_n^2/f_n$ as the coupling of the photon to the vector meson of mass m_n.

The existence of a state at $\sim \sqrt{3}\, m_\varrho$, long sought after the Veneziano model, is the first strong prediction of the model and a lack of observation of it would ruin many of the most important results, due to the sensitivity of the model to the parameter a, as we shall see in the following. The experimental implications concerning the $\varrho'(1250)$ are discussed in detail in Ref. 8. However, as main features, it should be identified with the $\omega\pi$ enchancement observed in photoproduction[13], with a small $\pi\pi$ branching ratio, and a strong contribution to $e^+e^- \to \omega\pi$ at $\sqrt{s} \simeq m_{\varrho'}$. Fortunately enough, there is already a clear deviation[14] from the Gounaris-Sakurai expression for $F_\pi(s)$ around $\sqrt{s} \sim 1.25$, and more recently, an experimental indication[15] of a strong $\omega\pi$ signal is e^+e^- annihilation in this energy region with a cross section of the order of $\sim$100 nbs. Clearly, further and more accurate data are needed to decide upon this vector state.

The process $e^+e^- \to$ hadrons at high energies is then pictured as proceeding by the virtual photon turning into vector mesons which then decay into hadrons. One has therefore:

$$\sigma_{had}(s) = \frac{12\pi}{s} \sum_n \frac{m_n^2 \Gamma_n \Gamma(V_n \to e^+e^-)}{(s - m_n^2)^2 + m_n^2 \Gamma_n^2}, \tag{2.2}$$

and forcing scaling with

$$\Gamma_n \alpha\, m_n, \qquad \frac{m_n^2}{f_n^2} = \text{const} = \frac{m_\varrho^2}{f_\varrho^2}, \tag{2.3}$$

one has the result

$$\sigma_{has}(s) \simeq \sigma_{\mu\bar{\mu}}(s) \frac{16\pi^2}{a f_\varrho^2}, \tag{2.4}$$

where $\sigma_{\mu\bar{\mu}}(s) = 4\pi\alpha^2/3s$ is the (pointlike) muon pair production cross section.

This gives, with a = 2,

$$R \equiv \frac{\sigma_{had}(s)}{\sigma_{\mu\bar{\mu}}(s)} = \frac{8\pi^2}{f_\varrho^2} \simeq 2.5. \qquad (2.5)$$

Equation (2.5) is quite interesting because it links together the asymptotic ratio R to a typical law energy parameter ($f_\varrho^2/4\pi$). This feature of the model is also common to what will be found in deep inelastic electron scattering, where the structure functions will be expressed in terms of photoproduction data for ϱ, ω and φ mesons, in very good agreement with experiment.

As is clear, the point-like behaviour of $\sigma_{tot}(e^+e^- \to \text{had})$ is provided in this picture by broader and broader higher mass vector mesons which add together to build up a smooth scaling continuum, in a very similar way to what happens in strong interactions, where an infinite number of resonances build up a smooth Regge-like behaviour of the scattering amplitude.

This analogy with strong interactions has been examined further by Sakurai[16]; who has conjectured a new "duality" between vector meson formation and scaling behaviour of the total cross section. More explicitly the following finite-energy sum rule has been suggested:

$$\int_{4m_\pi^2}^{s_{max}} sds \left[\sigma_{had}(s) - \sigma_{comp}(s)\right] = 0, \qquad (2.6)$$

where $\sigma_{had}(s)$ is the total cross section for e^+e^- annihilation into hadrons and $\sigma_{comp}(s)$ is a "comparison" cross section which approaches $\sigma_{had}(s)$ as $s \to \infty$ and is extrapolated down at low energies with appropriate threshold factors.

Eq. (2.6) is then used to predict the actual numerical value of the asymptotic ratio R defined above, by integrating (2.6) up to $s_{max} \simeq 1.2\ GeV^2$, and including in $\sigma_{had}(s)$ contributions of the well known ϱ, ω and φ mesons. By using for the comparison cross sectiont the following forms:

$$\sigma_{comp}(s) = R\frac{4\pi\alpha^2}{3s}\left(1+\frac{2m_\mu^2}{s}\right)\left(1-\frac{4m_\mu^2}{s}\right)^{1/2}, \qquad (2.7a)$$

$$\sigma_{comp}(s) = R\frac{4\pi\alpha^2}{3s}\left(1+\frac{2m_q^2}{s}\right)\left(1-\frac{4m_q^2}{s}\right)^{1/2}, \qquad (2.7b)$$

$$\sigma_{comp}(s) = R\frac{4\pi\alpha^2}{3s}\left(1-\frac{4m_\pi^2}{s}\right)^{3/2}, \qquad (2.7c)$$

with a "quark mass" $m_q = m_{N/3}$, the following values of R are found

$$R = 2.9, \tag{2.8a}$$

$$R = 5.0, \tag{2.8b}$$

$$R = 3.9. \tag{2.8c}$$

The above range of values of R reflects the uncertainties arising from the extrapolation of $\sigma_{comp}(s)$ to low energies. However a more general analysis based on a set of sum rules derived explicitly below, will confirm the value of R of eq. (2.5), in the same spirit of eq. (2.6).

2.2. Duality sum rules from canonical trace anomalies

In this section we derive[17] a complete set of sum rules relating the asymptotic ratio R to low energy moments of $\sigma(e^+e^- \to \text{hadrons})$, in the general framework of the canonical trace anomaly of the energy momentum tensor. This gives an exact mathematical formulation of duality in e^+e^- annihilation, in complete analogy to the familiar FESR of strong interactions.

Defining the Green functions

$$\Delta_{\mu\nu}(p, q) = \int d^4x d^4y\, e^{iqy} \langle 0 | T(\theta^\lambda_\lambda(x) J_\mu(y) J_\nu(0)) | 0 \rangle e^{ipx}, \tag{2.9}$$

and

$$\pi_{\mu\nu}(q) = i \int d^4x\, e^{iqx} \langle 0 | T(J_\mu(x) J_\nu(0)) | 0 \rangle, \tag{2.10}$$

where θ^λ_λ is the trace of the energy momentum tensor, Crewther[18] and Chanowitz and Ellis[19] have established the following anomalous trace identity

$$\Delta(q^2) = -2q^2 \frac{\partial \pi(q^2)}{\partial q^2} - \frac{e^2 R}{6\pi^2}, \tag{2.11}$$

with

$$\Delta_{\mu\nu}(q, 0) = (q_\mu q_\nu - g_{\mu\nu} q^2) \Delta(q^2),$$

$$\pi_{\mu\nu}(q) = (q_\mu q_\nu - g_{\mu\nu} q^2) \pi(q^2).$$

Since $\pi(q^2)$ is regular at $q^2 = 0$ one recovers from (2.11) the familiar result:

$$\Delta(0) = -\frac{e^2 R}{6\pi^2}. \tag{2.12}$$

On very general grounds $\Delta(q^2)$ is expected to vanish asymptotically for large q^2 x). One can therefore write for it an unsubtracted dispersion relation:

$$\Delta(q^2) = -\frac{2}{\pi} \int_{s_0}^{\infty} \frac{s \frac{\partial}{\partial s} \operatorname{Im} \pi(s)}{s - q^2} ds, \tag{2.13}$$

x) The usual argument[20] is that of Weinberg's theorem or the identification of θ^λ_λ with generalized mass terms in the Lagrangian.

where $\mathrm{Im}\,\pi(s)$ is related to the total e^+e^- annihilation cross section into hadrons by

$$\sigma_{had}(s) = \frac{4\pi\alpha}{s}\,\mathrm{Im}\,\pi(s). \tag{2.14}$$

A general form of $\mathrm{Im}\,\pi(s)$ which scales asymptotically is[x)]

$$\mathrm{Im}\,\pi(s) = f(s)\,\theta(s-s_o)\,\theta(\bar{s}-s) + \frac{\alpha}{3}\,R\,\theta(s-\bar{s}), \tag{2.15}$$

when inserted into (2.13) give the following q^2 structure

$$\Delta(q^2) = -\frac{2}{\pi}\,q^2\int_{s_o}^{\bar{s}}\frac{\mathrm{Im}\,\pi(s)ds}{(s-q^2)^2} - \frac{2\alpha}{3\pi}\,R\,\frac{\bar{s}}{\bar{s}-q^2}\,. \tag{2.16}$$

Expanding both sides of eq. (2.16) in inverse powers of q^2 and comparing coefficients one gets:

$$\int_{s_o}^{\bar{s}}\mathrm{Im}\,\pi(s)\,s^n\,ds = \frac{\alpha R}{3}\,\frac{\bar{s}^{n+1}}{n+1} - \frac{c_n}{n+1}\,, \tag{2.17}$$

where

$$q^2\,\Delta(q^2) \sim \frac{2}{\pi}\sum_{n=0}^{\infty} c_n\left(\frac{1}{q^2}\right)^n. \tag{2.18}$$

Eqs. (2.17) are nothing but the analogue of the familiar duality sum rules of strong interactions apart from the constants c_n. This is the exact mathematical formulation of duality in e^+e^- annihilation, where asymptotic scaling replaces the usual assumption of Regge behaviour. As can be seen from (2.17) the asymptotic value of R is directly connected to the low energy region of e^+e^- annihilation into hadrons.

An indirect determination of the constants c_n follows upon noting that by definition they have the dimensions of mass squared to the power (n+1) and thus have to depend homogeneously on a certain set of mass parameters $s_1, \ldots s_j$, which explicitly break scale invariance. Therefore the c_n satisfy the equation

$$\sum_j s_j\frac{\partial}{\partial s_j}\,c_n(s_1,\ldots s_j) = (n+1)\,c_n(s_1,\ldots s_j),$$

which together with eq. (2.17) yields.

$$\int_{s_o}^{\bar{s}}\left(1-\frac{1}{n+1}\sum_j s_j\frac{\partial}{\partial s_j}\right)\mathrm{Im}\,\pi(s_j,s)\,s^n\,ds = \frac{\alpha R}{3}\,\frac{\bar{s}^{n+1}}{n+1} \tag{2.19}$$

---

x) Contributions of non-leading terms of the form $(\alpha/3)R'(s'/s)^\beta\,\theta(s-\bar{s})$ are discussed in detail in Ref. 17. They do not change the essence of our results (see footnote after eq. 2.19).

where we have explicitly introduced the dependence of $\mathrm{Im}\,\pi$ on the mass parameters s_j [x].

As an example we consider now the model of section 1.1, where both $\Delta(q^2)$ can be explicitly calculated and the sum rules (2.19) take a simple form. In this case we have

$$\mathrm{Im}\,\pi(s) \sim 4\pi^2\alpha \sum_n \frac{m_n^2}{f_n}\,\delta(s-m_n^2) = 4\pi^2\alpha\,\frac{m_\varrho^2}{f_\varrho^2}\sum_n \delta(s-m_n^2) \tag{2.20}$$

and using (2.13) we find for the isovector contribution:

$$\Delta(q^2) - \Delta(0) = -\frac{e^2}{2f_\varrho^2}\,\frac{q^2}{m_\varrho^2}\,\zeta(2, 1/2 - q^2/2m_\varrho^2)\,, \tag{2.21}$$

where $\zeta(2,x)$ is the generalized Riemann zeta function defined as

$$\zeta(s,x) = \sum_{n=0}^{\infty} (x+n)^{-s}$$

From eq. (2.21) we obtain $\Delta(0) = -e^2/f_\varrho^2$ and therefore, through (2.12) and including isoscalars, $R = 8\pi^2/f_\varrho^2$ in agreement with our previous result. We can also explicitly evaluate the coefficients c_n appearing in (2.17) and find in particular $c_o = 0$. This last result can also be derived by observing that the derivative term on the r.h.s. of (2.19), with n=0, vanishes if $\mathrm{Im}\,\pi(s_j, s) \sim \delta(s-s_j)$, giving

$$\int_{s_o}^{\bar{s}} (\mathrm{Im}\,\pi(s) - \frac{\alpha R}{3})\,ds = 0, \tag{2.22}$$

as an identity in this model which is valid also locally. This follows from the fact that $\mathrm{Im}\,\pi(s)$ around any resonance of the series is of the form of eq. (2.20) and the effective range of integration is $2m_\varrho^2$ as given by the spacing of the mass spectrum. The value of R found this way ($R = 8\pi^2/f_\varrho^2$) is just the average of $3\,\mathrm{Im}\,\pi(s)/\alpha$ as low energies. This result is to be compared with that of Sakurai[16], (eqs. (2.6) and (2.7)), in which the uncertainties in the threshold factors of his $\sigma_{\mathrm{comp}}(s)$ give rise to corresponding uncertainties in R (eqs. 2.8).

In the light of above considerations it is interesting to comment on the experimental situation of e^+e^- annihilation. The local average of the data over the prominent

---

x) The inclusion of nonleading terms of the form $(\alpha/3)R'(s'/s)^\beta\,\theta(s-\bar{s})$ leads to

$$\int_{s_o}^{\bar{s}} (1 - \frac{1}{n+1}\sum_j s_j \frac{\partial}{\partial s_j})\,\mathrm{Im}\,\pi(s_j, s)\,s^n\,ds = \frac{\alpha}{3}\,\bar{s}^{n+1}\left\{R + R'(s'/\bar{s})^\beta\right\}$$

resonances ($\varrho, \omega, \varphi, \varrho', \ldots$) is approximately constant (~ 2.5) and agrees with the value of R found experimentally for q^2 up to about 10 GeV^2 [21]. This is in agreement with our predictions and the duality sum rule (2.22), thus indicating the presence of a component of Im $\pi(s)$ which scales precociously.

From $q^2 \gtrapprox 10$ to about 25 GeV^2 R apparently increases linearly with q^2 [4]. This suggests the presence of a new component in Im $\pi(s)$, with threshold at $s \gtrapprox 10$ GeV^2, additive to the previous one and possibly responsible also for the violations of scaling observed at small x in the single inclusive distributions. The observed scaling behaviourof the same distributions at large x is indeed in accord with our theoretical expectations, as discussed in detail in the next section. More on the new component of Im $\pi(s)$ can be found at the end of section 3.1.

2.3. Threshold behaviour of pion distributions [22].

As shown in Fig. 1 the recent SPEAR data have indicated that the inclusive distribution behaves quite differently in the x region explored. In addition to the large violation of scaling observed for $x \equiv \frac{2E}{\sqrt{q^2}} \lesssim 0.5$ which reflects itself into the rise of R, the data [4] are quite consistent with $q^2 d\sigma/dx$ scaling for $x \gtrsim 0.5$, giving also evidence for an essential isotropy of the angular distributions. Furthermore, the pion structure function near $x = 1$ is more than an order of magnitude larger than the proton one, as measured in deep inelastic electron-proton scattering.

This striking result is however in excellent agreement with a prediction made some time ago [23], based on the use of Bloom-Gilman type FESR [24] together with an EVMD model for the pion form factor $F_\pi(s)$. We briefly discuss this result, and more generally study the longitudinal and transverse structure functions for both charged and neutral pions. The single inclusive differential cross section may be written in terms of the usual structure functions $\bar{F}_1$ and $\bar{F}_2$ as:

$$\frac{d\sigma}{dx\,dz} = \frac{\pi\alpha^2}{2s}\sqrt{x^2 - \frac{4\mu^2}{s}}\left\{2\bar{F}_1(x,s) + \frac{1}{2x}\left(x^2 - \frac{4\mu^2}{s}\right)(1-z^2)\bar{F}_2(x,s)\right\} \qquad (2.23)$$

where $q^2 = s$, μ is the pion mass and z is the cosine of the angle made by the pion with respect to the e^+e^- beam. For later purposes, it is more convenient to introduce longitudinal and transverse structure functions as follows:

$$\frac{d\sigma}{dx\,dz} = \frac{\pi\alpha^2}{2s}\sqrt{x^2 - 4\mu^2/s}\left\{F_T(x,s)(1+z^2) + F_L(x,s)(1-z^2)\right\}. \qquad (2.24)$$

The cross section for pion paris production is given by:

$$\frac{d\sigma(e^+e^- \to \pi^+\pi^-)}{dz} = \frac{\pi\alpha^2}{4s}\left(1 - \frac{4\mu^2}{s}\right)^{3/2} |F(s)|^2 (1-z^2). \qquad (2.25)$$

For large s, assuming scaling and a threshold behaviour $F_L(x) \sim c_\pi (1-x)^2$, which are both consistent with the present data, Bloom-Gilman FESR gives:

$$\frac{1}{s} \int_{\mu^2}^{\sim m_\varrho^2} F_L(x,s)\, dM_x^2 \approx \int_{1-\frac{1}{s}(m_\varrho^2-\mu^2)}^{1} F_L(x)\, dx, \qquad (2.26)$$

which implies

$$|F_\pi(s)|^2 \underset{\text{large s}}{\sim} \frac{2}{3} c_\pi \left(\frac{m_\varrho^2}{s}\right)^3 . \qquad (2.27)$$

A model for $F_\pi(s)$, with such an asymptotic behaviour has been explicitly constructed[23] using EVMD. It is found:

$$|F_\pi(s)| \underset{\text{large s}}{\sim} 3 \left(\frac{m_\varrho^2}{s}\right)^{3/2} , \qquad (2.28)$$

which, together with (2.27) gives $c_\pi \simeq 27/2$. By using the experimental information that $F_L^{(\pi^+)}(x) \simeq F_T^{(\pi^+)}(x)$ we finally predict:

$$\frac{d\sigma(e^+e^- \to \pi^+ + x)}{dx} \underset{x \approx 1}{\sim} 27 \frac{\pi\alpha^2}{s} (1-x)^2 , \qquad (2.29)$$

which is in excellent agreement with the data, for $x \gtrsim 0.5$. This result shows that the observed scaling behaviour of the pion structure function, for large values of x, agrees with our expectations based on simple duality arguments. This is also supported by the following analysis of the transverse structure functions.

The main contributions to the transverse structure function for π^o and π^+ production near threshold come from the exclusive processes $e^+e^- \to \pi^o\omega$ and $e^+e^- \to \pi^+ A_2^-$ respectively. The corresponding cross sections are given by:

$$\frac{d\sigma(e^+e^- \to \pi^o\omega)}{dx\, dz} = \left(\frac{\pi\alpha^2}{16}\right)\left(x^2 - \frac{4\mu^2}{s}\right)^{3/2} |G_{\omega\pi\gamma}(s)|^2 (1+z^2)\,\delta\left(1 - \frac{m_\omega^2 - \mu^2}{s} - x\right), \qquad (2.30)$$

$$\frac{d\sigma(e^+e^- \to \pi^+ A_2^-)}{dx\, dz} = \left(\frac{\pi\alpha^2}{16}\right)\left(x^2 - \frac{4\mu^2}{s}\right)^{5/2} |G_{A_2\pi\gamma}(s)|^2 \frac{s^2}{8 m_{A_2}^2} (1+z^2)\,\delta\left(1 - \frac{m_{A_2}^2 - \mu^2}{s} - x\right), \qquad (2.31)$$

where $G_{\omega\pi\gamma}(s)$ and $G_{A_2\pi\gamma}(s)$ are the transition form factors which are normalized at $q^2 \equiv s = 0$ to the corresponding radiative decay widths:

$$\Gamma_{\omega \to \pi^o\gamma} = \frac{|G_{\omega\pi\gamma}^2(0)|^2}{4\pi} \frac{P_\pi^3}{3} , \quad \Gamma_{A_2 \to \pi\gamma} = \frac{|G_{A_2\pi\gamma}^2(0)|^2}{4\pi} \frac{P_\pi^5}{20} .$$

In order to exploit the duality sum rules as in (2.26), one needs to know the asymptotic behaviour of the form factors which appear in eqs. (2.30) and (2.31). This has been done in Ref. 22, by using a modified Harary-Pagels sum rule for virtual compton photon on pions. As a result the following relations are obtained

$$\left| \frac{G_{\omega\pi\gamma}(Q^2)}{G_{A_2\pi\gamma}(Q^2)} \right|^2 \underset{Q^2 \text{large}}{\sim} \frac{(Q^2)^2}{8\, m^2_{A_2}}, \tag{2.32}$$

and

$$\left| \frac{G_{\omega\pi\gamma}(Q^2)}{F_\pi(Q^2)} \right|^2 \underset{Q^2 \text{large}}{\sim} \frac{4}{Q^2}. \tag{2.33}$$

Thus we are finally able to estimate the transverse structure functions near threshold, via duality sum rule. We obtain, near $x = 1$,

$$\frac{1}{s}\int F_T^{(\pi^o)}(x,s)\, dM_x^2 \simeq \frac{1}{8}\int s \left| G_{\omega\pi\gamma}(s) \right|^2 \delta\left(1 - \frac{m_\omega^2 - \mu^2}{s} - x\right) \simeq \int F_T^{(\pi^o)}(x)\, dx, \tag{2.34a}$$

$$\frac{1}{s}\int F_T^{(\pi^+)}(x,s)\, dM_x^2 \simeq \frac{1}{8}\int \frac{s^3}{8\, m^2_{A_2}} \left| G_{A_2\pi\gamma}(s) \right|^2 \delta\left(1 - \frac{m^2_{A_2} - \mu^2}{s} - x\right) \simeq \int F_T^{(\pi^+)}(x)\, dx, \tag{2.34b}$$

$$\frac{1}{s}\int F_L^{(\pi^+)}(x,s)\, dM_x^2 = \frac{1}{2}\int \left| F_\pi(s) \right|^2 \delta(1-x) \simeq \int F_L^{(\pi^+)}(x)\, dx, \tag{2.34c}$$

and through eqs. (2.31) and (2.33),

$$F_L^{(\pi^+)}(x) \simeq F_T^{(\pi^+)}(x) \simeq F_T^{(\pi^o)}(x) \simeq c_\pi (1-x)^2. \tag{2.35}$$

We therefore predict an almost isotropy in the π^+ inclusive angular distributions, in agreement with data.

As far as π^o production is concerned, due to the absence of the pion pole, as well as the absence of important exclusive channels contributing to $F_L^{(\pi^o)}(x)$ near $x=1$, we predict at threshold essentially a transverse component. Experimental checks on this point will be very important for duality ideas.

We conclude this paragraph by summarizing our basic results. In addition to describing the prominent resonances observed at low energies, the model presented given an intuitive picture of scaling, with the appealing feature of connecting the asymptotic ratio R to the low energy parameter $(f_\varrho^2/4\pi)$. Furthermore we have proved this "dual" connection, in the sense of FESR, to be true on much more general grounds, suggesting also the presence of a precociously scaling component of $\mathrm{Im}\,\pi(s)$ essentially

from threshold to the highest values of s experimentally explored. The same model has been then successfully used to account for the observed scaling behaviour of the pion distribution function, helped by Bloom-Gilman type sum rules. The big question which is still open, is of course the origin of the non-scaling component in $\mathrm{Im}\,\pi(s)$ which, following the above analysis, seems to have a threshold at $s \simeq 10\ \mathrm{GeV}^2$. Further experimental informations on the exclusive structure of the hadrons produced will be of great help for answering this question, particularly in connection with many theoretical attempts to enlighten the experimental situation.

3. PHOTO- AND ELECTRO-PRODUCTION.

3.1. Scattering of photons off nucleons.

The failure of the vector dominance model in relating the cross-section for photoproduction of vector meson to the total hadronic photon nucleon cross-section is well known. More explicitly, using the relation[13]

$$\sigma_{tot}(\gamma p) = \sum_{V=\varrho,\omega,\varphi} \sqrt{\frac{16\pi^2 e^2}{f_V^2} \frac{1}{1+\eta_V^2} \frac{d\sigma^o}{dt}(\gamma p \to Vp)} \qquad (3.1)$$

where $d\sigma^o/dt$ denotes the forward cross-section, and η_V the ratio of the real to the imaginary parts, the value of $f_\varrho^2/4\pi$ obtained through eq. (3.1) from photoproduction data is smaller by a factor of about two than the results from e^+e^- colliding beams. We will show in detail that eq. (3.1) can be exactly satisfied in the framework of our model, determining in addition the exact density of the vector mass spectrum.

We shall assume[8] the well-known two-component duality framework in which the ordinary Regge exchanges and the Pomeron exchange average the resonances and the background respectively. The total photoabsorption cross-section can then be written in terms of a diffractive and resonance contribution, and is parametrized as follows[13]:

$$\sigma_{\gamma p}(\nu) \equiv \sigma^D_{\gamma p} + \sigma^R_{\gamma p}(\nu) = 98.7 + \frac{64.9}{\sqrt{\nu}} \quad (\mu b)\,. \qquad (3.2)$$

Defining

$$\sigma_{\varrho p}(\nu) = \sqrt{\frac{16\pi}{e^2} f_\varrho^2 \frac{1}{1+\eta_\varrho^2} \frac{d\sigma^o}{dt}(\gamma p \to \varrho p)} \qquad (3.3)$$

with an analogous separation into diffractive and resonant terms, the inclusion of the set of vector states leads to the following extensions of (3.1) for both diffractive and resonant components:

$$\sigma^D_{\gamma p} = \frac{4\pi\alpha}{f_\varrho^2}\ \sigma^D_{\varrho p} \sum_n \frac{1}{1+an} \frac{\sigma^D_{np}}{\sigma^D_{\varrho p}} + \text{isoscalars}\,, \qquad (3.4a)$$

$$\sigma^{R}_{\gamma p}(\nu) = \frac{4\pi\alpha}{f_\varrho^2}\ \sigma^{R}_{\varrho p}(\nu)\ \sum_n \frac{1}{1+an}\ \frac{\sigma^{R}_{np}(\nu)}{\sigma^{R}_{\varrho p}(\nu)} + \text{isoscalars}, \qquad (3.4b)$$

where we have used for all n the previous result $m_n^2/f_n^2 \simeq m_\varrho^2/f_\varrho^2$, and the isoscalars account for both ω-like and φ-like production. In writing eqs. (3.4) we have explicitly assumed the validity of a diagonal approximation for the forward imaginary part of the vector dominated Compton amplitude. For the diffractive part this is supported by the dominance of diagonal Pomeron couplings over off-diagonal ones in two-body and quasi-two-body hadronic processes. In addition, the value of $f_\varrho^2/4\pi$ obtained in this approximation from forward ϱ-photoproduction is in good agreement with the storage rings value. As far as the non-diffractive part is concerned, we will take it as a working hypothesis and check its validity a posteriori.

As it is clear, a reason of simplicity is also at the origin of assuming, in the average, the diagonal approximation. The actual relevance of possible off-diagonal contributions depends on the specific form and the free parameters introduced, without any predictive power[x].

Let us consider eq. (3.4a). To proceed further we need the purely strong interaction cross-sections σ^{D}_{np}. We will fix them by naive dimensional analysis, i.e., $\sigma^{D}_{n} \sim 1/m_n^2$. In Regge language, this impies for the forward elastic $(V_n p)$ amplitude A_n:

$$A_n \sim \Sigma_i \left(\frac{s}{m_n^2}\right)^{\alpha_i}\ \beta_i \qquad (3.5)$$

with the same β_i for all n. Such a scaling behaviour of strong interactions has been shown by Rittenberg and Rubinstein[26], in the framework of dual resonance models[o]. We finally obtain:

$$\sigma^{D}_{\gamma p} = \frac{11}{9}\ \frac{4\pi\alpha}{f_\varrho^2}\ \sigma^{D}_{\varrho p}\ \frac{1}{a^2}\ \zeta\left(2, \frac{1}{a}\right) \qquad (3.6)$$

where a factor 2/9 accounts for the isoscalars production. ($\sigma_{\varrho N} = \sigma_{\omega N} \simeq 2\,\sigma_{\varphi N}$). Using photoproduction data[13] (3.6) holds with a = 2, the correction to the pure VDM result being 23%. The mass spectrum of the vector states coupled to the photon is therefore pure Veneziano-like, as stated earlier. Equation (3.4b), augmented by eq. (3.5) is now a prediction of the model and provides a useful check for both the diagonal approximation and for our statements on the m_n^2 dependence of the Regge residues. We

---

x) An explicit model for off-diagonal contributions is discussed in the Schildknecht lecture[25].

o) The behaviour $\sigma_n \sim m_n^{-2}$ is of great relevance for the absence of shadowing effects on nuclei at large q^2. See the detailed discussion in next section.

obtain

$$\sigma^{R}_{\gamma p}(\nu) = \frac{11}{9}\,\frac{4\pi\alpha}{f_\varrho^2}\,\sigma^{R}_{\varrho p}(\nu)\,\frac{1}{2^{3/2}}\,\zeta\left(\frac{3}{2},\frac{1}{2}\right) \tag{3.7}$$

which gives a 69% correction to the VDM, and is in excellent agreement with the data [both sides of (3.7) agree within $\sim 5\%$].

We have shown how the actual situation existing in photoproduction can be sensibly improved within the framework of our picture, providing also agreement with the colliding beam results. As seen above, moderate but significant corrections arise from the continuum of higher mass states at $q^2 = 0$. In deep inelastic scattering, as discussed below, the continuum will be responsible for the observed scaling behaviour of the structure functions, giving also a nice description of the data.

Let us now discuss electron-proton scattering, particularly in the deep inelastic region. Recall the definition of the structure functions $W_1(\nu, q^2)$ and $W_2(\nu, q^2)$ in terms of the transverse and longitudinal virtual photon cross-sections $\sigma_T(\nu, q^2)$ and $\sigma_L(\nu, q^2)$:

$$W_1(\nu, q^2) = \frac{1}{4\pi^2\alpha}\left(\nu - \frac{q^2}{2M}\right)\sigma_T(\nu, q^2), \tag{3.8a}$$

$$W_2(\nu, q^2) = \frac{1}{4\pi^2\alpha}\left(\nu - \frac{q^2}{2M}\right)\frac{q^2}{q^2+\nu^2}\left[\sigma_T(\nu, q^2) + \sigma_L(\nu, q^2)\right], \tag{3.8b}$$

where M is the proton mass. Let us separate the transverse cross-section $\sigma_T(\nu, q^2)$ into diffractive and resonant part, as previously done at $q^2=0$. The obvious generalization of eqs. (3.4) gives:

$$\sigma^{D}_{T}(\nu, q^2) = \frac{4\pi\alpha}{f_\varrho^2}\left(1-\frac{1}{\omega}\right)\sigma^{D}_{\varrho p}\sum_n \frac{1}{\left(\frac{q^2}{m_\varrho^2}+1+2n\right)^2} + \text{isoscalars}, \tag{3.9a}$$

$$\sigma^{R}_{T}(\nu, q^2) = \frac{4\pi\alpha}{f_\varrho^2}\left(1-\frac{1}{\omega}\right)\sigma^{R}_{\varrho p}(\nu)\sum \frac{(1+2n)^{1/2}}{\left(\frac{q^2}{m_\varrho^2}+1+2n\right)^2} + \text{isoscalars}, \tag{3.9b}$$

where as usually $\omega = 2M\nu/q^2$ ($q^2 > 0$). Let us discuss separately the two contributions. Equation (3.9a) can be rewritten as

$$\sigma^{D}_{T}(\nu, q^2) = \frac{\pi\alpha}{f_\varrho^2}\left(1-\frac{1}{\omega}\right)\sigma^{D}_{\varrho p}\,\zeta\left(2, \frac{q^2}{2m_\varrho^2}+\frac{1}{2}\right) + \text{isoscalars}, \tag{3.10}$$

which asymptotically behaves as

$$\sigma^{D}_{T}(\nu, q^2) \underset{q^2\to\infty}{\sim} \frac{2\pi\alpha}{f_\varrho^2}\left(1-\frac{1}{\omega}\right)\sigma^{D}_{\varrho p}\,\frac{m_\varrho^2}{m_\varrho^2+q^2} + \text{isoscalars}. \tag{3.11}$$

From (3.9b) we similarly obtain

$$\sigma_T^R(\nu,q^2) \underset{q^2\to\infty}{\sim} \frac{\pi^2\alpha}{f_\varrho^2}\left(1-\frac{1}{\omega}\right)^{1/2} \sigma_{\varrho p}^R(\nu)\sqrt{\frac{m_\varrho^2}{m_\varrho^2+q^2}} + \text{isoscalars}. \tag{3.12}$$

The transverse parts of the structure function is finally given by

$$\nu W_{2T}^D(\nu,q^2)\to \frac{11}{9}\frac{1}{\pi}\frac{m_\varrho^2}{2f_\varrho^2}\sigma_{\varrho p}^D\left(1-\frac{1}{\omega}\right)^2 \to 0.22, \tag{3.13a}$$

$$\nu W_{2T}^R(\nu,q^2)\to \frac{11}{9}\frac{m_\varrho}{4f_\varrho^2}\sqrt{q^2}\,\sigma_{\varrho p}^R(\nu)\left(1-\frac{1}{\omega}\right)^{3/2} \to 0.3\,\frac{1}{\sqrt{\omega}}. \tag{3.13b}$$

We would like to emphasize that our results are pure predictions of the model, with no use of adjustable parameters. Let us discuss them in detail. In the framework of two-component duality we have shown that starting from Regge behaved meson proton cross-sections, scaling results for νW_2 naturally arise once a similar scaling behaviour is also shared by purely strong forward amplitudes, namely $A_n \sim \Sigma_i s^{\alpha_i}\beta_i(m_n^2)$ with $\beta_i(m_n^2)\sim(1/m_n^2)^{\alpha_i}$ [eq. (3.5)]. We recall that this follows from the n dependence of the couplings f_n as inferred from e^+e^- scaling. Furthermore we have been able to construct the structure functions explicitly, starting only with a knowledge of the photoproduction data for the ϱ, ω and φ mesons. The precocious onset of scaling is evident from eqs. (3.11) and (3.12), since m_ϱ^2 fixes the scale of the momentum transfer. On the other hand, as follows from eqs. (3.13), the threshold behaviour is quite poor, the reason being simply due to the lack of any low energy ($s\sim m_n^2$) resonant behaviour in the Regge-like expressions of σ_n.

Equations (3.9) and (3.13) are plotted in Figures 2 and 3 and compared with experiments. The presence of a longitudinal contribution is accounted for by multiplying $\nu W_{2T}^D(\omega)$ by a factor 1.2. As one sees the agreement is exceptionally good, especially if one bears in mind that eqs. (3.13) are absolute predictions of the model.

A few words about the longitudinal cross-sections $\sigma_L(\nu,q^2)$ are in order here. The naive extrapolation in q^2 from $q^2=0$ leads, as is well known, to a logarithmic growth in q^2, and therefore to a breakdown of scaling. On the other hand, it is a basic assumption of vector dominance that certain matrix elements are smooth, which is actually quite ambiguous as the choice of the particular set of extrapolation functions is not a priori obvious. In fact, it has been shown[27] that on the basis of only gauge invariance and analyticity the commonly accepted statement $\sigma_L^V/\sigma_T^V \sim \zeta q^2/m_V^2$ is not a general feature of the model; other forms for σ_L^V/σ_T^V are also possible which preserve Bjorken's scaling. For example, if, just for fun, we assume $\sigma_L^V/\sigma_T^V \sim \zeta q^2/(m_V^2+q^2)$ then scaling is easily obtained in analogy to (3.11) and (3.12). Thus in the absence of a dynamical

statement concerning σ_L^V, we have simply taken it into account by using the experimental ratio $R = \sigma_L/\sigma_T \simeq 0.2$ [x].

We discuss now our results in connection with e^+e^- annihilation, in particular in the light of the considerations of section 2.2. Eqs. (3.4) and (3.9) are a particular case of a more general picture in which one considers the photon fluctuating into its hadronic constituents, which subsequently interact with the target[28]. One easily obtains in this case

$$\sigma_T(\nu, q^2) = \frac{1}{\pi} \int_{s_o}^{\infty} \frac{\mathrm{Im}\,\pi(s)\, s}{(s+q^2)^2}\ \sigma_{had}(s, \nu)\, ds, \tag{3.14}$$

where $\sigma_{had}(s, \nu)$ is the cross section for the hadronic system of mass s to interact with the target with a given energy ν. In our model, using the expression (2.20) for Im $\pi(s)$ one simply recovers from (3.14) the eqs. (3.4) and (3.9).

We shall use now the idea of precocious scaling of Im $\pi(s)$ by, writing in (3.14) $\mathrm{Im}\,\pi(s)^{(I=1)} = 4\pi^2\alpha\ m_\varrho^2\ \delta(s-m_\varrho^2)/f_\varrho^2 + 2\alpha\pi^2\theta(s-2m_\varrho^2)/f_\varrho^2$, namely by considering (3.14) as given by the simple ϱ pole contribution (ω and φ for isoscalars) added to a scaling contribution with $\mathrm{Im}\,\pi(s) = \alpha R/3$, R being $6\pi^2/f_\varrho^2$ for the isovector component (an overall factor 4/3 takes then into account also isoscalars)[o]:

$$\sigma_T^{I=1}(\nu, q^2) = \frac{4\pi\alpha}{f_\varrho^2}\ \frac{m_\varrho^4}{(m_\varrho^2+q^2)^2}\ \sigma_\varrho(\nu) + \frac{2\pi\alpha}{f_\varrho^2} \int_{2m_\varrho^2}^{\infty} \frac{s\,\sigma_{had}^{I=1}(s, \nu)}{(s+q^2)^2}\, ds, \tag{3.15}$$

where the lower limit of the integral is half between the ϱ and the ϱ' ($m_{\varrho'}^2 = 3m_\varrho^2$). With the usual separation into a diffractive a resonant component and using again our scaling prescriptions $s\,\sigma_{had}^D(s) = m_\varrho^2\,\sigma_\varrho^D$ and $s\,\sigma_{had}^R(s, \nu) = m_\varrho\sqrt{s}\ \sigma_\varrho^R(\nu)$ one easily finds

$$\sigma_T^D(q^2) = \frac{4\pi\alpha}{f_\varrho^2}\ \frac{m_\varrho^4}{(m_\varrho^2+q^2)}\ \sigma_\varrho^D + \frac{2\pi\alpha}{f_\varrho^2}\ \frac{m_\varrho^2}{2m_\varrho^2+q^2}\ \sigma_\varrho^D + \text{isoscalars}, \tag{3.16a}$$

$$\sigma_T^R(\nu, q^2) = \frac{4\pi\alpha}{f_\varrho^2}\ \frac{m_\varrho^2}{(m_\varrho^2+q^2)^2}\ \sigma_\varrho^R(\nu) + \frac{2\pi\alpha}{f_\varrho^2}\ m_\varrho\ \sigma_\varrho^R(\nu) \left\{ \frac{\pi}{2}\ \frac{1}{\sqrt{q^2}} - \right.$$
$$\left. - \frac{1}{\sqrt{q^2}}\ \mathrm{arctg}\sqrt{\frac{2m_\varrho^2}{q^2}} + \frac{\sqrt{2m^2}}{2m_\varrho^2+q^2} \right\} + \text{isoscalars}. \tag{3.16b}$$

For photoproduction one then gets

---

x) See also the discussion following eq. (4.4), concerning the limiting value of R, as $\omega \to \infty$.
o) See also Ref. 9.

$$\sigma_\gamma^D = \frac{4\pi\alpha}{f_\varrho^2}\,\sigma_\varrho^D\left(1+\frac{1}{4}\right) + \text{isoscalars}, \tag{3.17a}$$

$$\sigma_\gamma^R(\nu) = \frac{4\pi\alpha}{f_\varrho^2}\,\sigma_\varrho^R(\nu)\left(1+\frac{1}{\sqrt{2}}\right) + \text{isoscalars}, \tag{3.17b}$$

in excellent agreement with (3.6) and (3.7), while in deep inelastic scattering ($q^2 \to \infty$) eqs. (3.16) give

$$\sigma_T(\nu, q^2) \sim \frac{2\pi\alpha}{f_\varrho^2}\,\frac{m_\varrho^2}{q^2}\,\sigma_\varrho^D + \frac{\pi^2\alpha}{f_\varrho^2}\,\sigma_\varrho^R(\nu)\sqrt{\frac{m_\varrho^2}{q^2}} + \text{isoscalars}, \tag{3.18}$$

which coincides with (3.11) and (3.12). It follows therefore that the idea of precocious scaling in e^+e^- annihilation is perfectly consistent both with our previous analysis based on the vector meson spectrum and with experimental data in the space-like region. Furthermore, in the framework of eq. (3.14), one gets for consistently definite limitations on the high energy behaviour of the second component of Im π (s), i.e. that responsible for the rising of R, with threshold at $s \simeq 10$ GeV^2, as discussed in detail in section 2.2.

By comparing (2.16) with the diffractive component of (3.14), with $s\,\sigma_{had}^D(s) \sim$ $\sim$const, one finds for the isovector part

$$-\Delta(0) = \frac{e^2 R}{6\pi^2} = \lim_{q^2\to\infty} \frac{2q^2\,\sigma_T(q^2)}{m_\varrho^2\,\sigma_\varrho}. \tag{3.19}$$

In our model this relation is identically satisfied (see eqs. (2.21) and (3.10)) with $R = 8\pi^2/f_\varrho^2$ and is in agreement with the present observed value of νW_2. An asymptotic value of R larger than ~ 2.5, for example $R \simeq 5 \div 6$, would imply in our picture a corresponding increase of the limiting value of νW_2, in constrast with the experimental evidence at NAL[29]. Therefore if the observed increase of R is a genuine one-photon effect, we are led to expect

$$\int_{\sim 10\ \text{GeV}^2}^{\infty} \left(\text{Im}\,\pi(s) - \frac{\alpha}{3}\,\frac{8\pi^2}{f_\varrho^2}\right) ds \simeq 0, \tag{3.20}$$

in other words the new component of Im π(s) has to average to zero at higher energies. This ultimate result is another typical example (recall also a=2) of how tightly the model is constrained from the links among different processes in both space like and time like regions.

3.2. Scattering of photons off nuclei-Shadowing.

The propagation of light through nuclear matter shows clear evidence for hadron like behaviour of the photon. It is well known in fact that the A dependence of

total photon-nucleus cross sections is slower than $\sim A$. This shadowing effect[30] has been both experimentally[31] and theoretically[30,32] studied in great detail and provides indeed a rather sensitive test of VMD. The physical origin of this effect has been discussed many times and can be easily found in the literature[33]. It is simply related to the virtual transitions of the photon into its hadronic constituents and the amount of the corresponding propagation according to their mean free path in nuclear matter.

Although qualitatively explained by VMD, this effect has been however a source of some embarrassment to the traditional vector dominance people in the following sense. The vector dominance model was shown in Refs. 32 and 33, to lead to considerable shadowing at sufficiently high energies. This is indeed true experimentally for real photons ($q^2=0$) and energies $\nu \gtrsim$ 2-3 GeV, although pure VMD predicts considerably more shadowing than observed[34]. But the shadowing effect seems to disappear dramatically with q^2. For example, we quote a typical figure[34]: for gold (A=197), at $\nu \simeq 3$ to 8 GeV, the relevant ratio $S \equiv \sigma^{\gamma A}/A\,\sigma^{\gamma N} \simeq 0.65$ at $q^2 = 0$, and is $\simeq 1$ for $0.25 \leq q^2 \leq$ ≤ 0.75 GeV/c. Such a sharp change in S with q^2 is difficult to bring about in VMD and this has been hailed by some to provide the coup de grace to the (old) vector dominance model.

In EVMD the situation is much better. In fact, the same mechanism which helps to obtain Bjorken scaling in "γ p" scattering also alleviates this failing in "γ"-nucleus scattering. Qualitatively, the criterion for shadowing is given by

$$\frac{M_V^2 + q^2}{\nu}\, l_V \ll 1, \qquad (3.21)$$

where l_V is the mean free path of the vector meson V in nuclear matter ($l_V \propto 1/\sigma_{VN}$). Now Bjorken-scaling in EVMD is obtained by having the higher mass vector states become more and more important as q^2 increases. This, through the above equation, leads us immediately to the conclusion that shadowing is shifted to higher energies (larger ν) as q^2 increases.

There are however two different approaches[8,9] in EVMD for photo- and electroproduction on nucleons which basically differ in the choice of coupling the n-th vector meson to the photon and the vector meson-hadron cross sections. These two approaches lead to two different predictions concerning the high energy behaviour of the shadowing effect. More in detail, in our approach $\sigma_n \sim 1/m_n^2$ (see eq. (3.5) and related discussion) and therefore the corresponding l_n becomes unbounded for the n-th vector meson as $n \to \infty$, leading thus to the prediction that for q^2 large no shadowing takes place[35]. In the other approach[9] $\sigma_n \sim$ const, and therefore the shadowing effect comes back for large fixed q^2 as ν is sufficiently large[36].

For moderate values of ν and q^2 ($\nu \approx 20$ GeV, $q^2 \lesssim 1.5$ GeV^2) both approaches however agree within (10+20)% and bring theory in much better agreement with experiments[x] than pure VMD. The overall situation is summarized in Figs. 4, 5 and 6.

The details of the calculations are not discussed in detail here. The reader can easily go through them in the original papers. We give here only the results[35] of our approach in the limit $\nu \to \infty$, A large:

$$\frac{\sigma_{\gamma A}(\nu)}{A\,\sigma_{\gamma N}(\nu)} \simeq \frac{3}{2}\,\frac{l_\varrho}{2}\,(1+20\%), \quad \text{at } q^2=0, \tag{3.22}$$

where l_ϱ is the ϱ-meson mean free path ($l_\varrho \simeq 3$ fm) and R is the nuclear radius;

$$\frac{\sigma_{\gamma A}(\nu, q^2)}{A\,\sigma_{\gamma N}(\nu, q^2)} \xrightarrow[\nu/q^2 \text{ fixed}]{\text{large } \nu,\ q2} 1 - H(q^2), \tag{3.23}$$

where $H(q^2)$ is given by

$$H(q^2) \simeq \frac{2}{(1+q^2/m_\varrho^2)}\left(1-\frac{3l_\varrho}{2R}\right)+\frac{3R}{8l_\varrho}\left(1+\frac{m_\varrho^2}{q^2}\right)\left\{\frac{m_\varrho^2}{q^2}\ln\left(1+\frac{q^2}{3m_\varrho^2}\right)-\frac{m_\varrho^2}{q^2+3m_\varrho^2}\right\} \tag{3.24}$$

The accuracy of (3.24) is still good at $q^2 \gtrsim 1$ GeV^2, provided the energy is large enough ($\nu \gtrsim 100$ GeV). At lower energies one has both to take into account non-diffractive contributions to the cross sections which are not included in (3.24) and use the exact expressions, which can be worked out only numerically.

To conclude, we have shown that our model provides a nice description of the observed features of the ν, q^2 and A dependence of the photon-nuclei cross sections. We predict that for large q^2 no shadowing takes place, in contrast with the predictions made in Ref. 36. Of course further and more accurate experimental data on the q^2 dependence would be highly desirable, particularly at large energies. It has to be emphasized that this kind of experiments provides a crucial test for the scaling hypothesis of the hadronic cross-sections.

4. DEEP INELASTIC NEUTRINO-NUCLEON SCATTERING[10]

We would like to discuss now neutrino and antineutrino-scattering into hadrons by extending to these processes the results previously obtained in photo-and electroproduction. In particular we will be able to reproduce all the results of the quark parton model without invoking point constituents, determining in addition the weak struc-

---

x) In this connection see the interesting comments by G. Grammer in the discussion session, pointing out that shadowing emerges clearly once radiative corrections are taken into account at various q^2.

ture functions by means of the usual tools of hadron physics.

Let's start by recalling that in section 3.1 we were able to determine the photoproduction cross sections and deep inelastic e N scattering in terms of ϱN cross section. This is measured in ϱ-photoproduction and agrees pretty well both in magnitude and ν dependence with the average of the $\pi^{\pm}$N cross sections[13]. This identifications, as well known, is a nice prediction of the simple quark model[37]. Using this fact, we have a first simple connection among quite different processes as πN scattering, ϱ and total photoproduction and deep inelastic eN scattering. A similar relation was derived by Langacker and Suzuki[38] and Fujikawa and O'Donnell[39]. More in detail, the total cross section for πN scattering is related through PCAC to the structure function F_2^A for the axial vector current:

$$\sigma_{\pi N}(\nu) = \frac{\pi}{f_\pi^2} F_2^A(\nu, q^2=0), \tag{4.1}$$

where f_π is the pion decay constant. Furthermore, from the Deser-Gilbert-Sudarshan representation Langacker adn Suzuki also showed that the Pomeron residue of F_2^A is independent of q^2, whence

$$\sigma_{\pi N}(\infty) = \frac{\pi}{f_\pi^2} F_2^A(\infty), \tag{4.2}$$

having assumed Bjorken scaling for $F_2^A(\nu, q^2)$. On the other hand, taking into account only the isovector contribution in eq. (3.13a) we have

$$\sigma_{\pi N}(\infty) = \pi \frac{2f_\varrho^2}{m_\varrho^2} F_2^V(\infty). \tag{4.3}$$

By comparing (4.2) and (4.3) and using the chiral relation $F_2^A = F_2^V$, we derive

$$2 f_\varrho^2 f_\pi^2 = m_\varrho^2 , \tag{4.4}$$

the well known SKFR relation[40], which is experimentally verified with very good accuracy. This result strongly supports our picture of deep inelastic eN scattering which leads to eqs. (3.13). It also reinforces Pagels's conjecture[41] of the fundamental role played by f_π as the dimensional constant in strong interactions. Conversely, by assuming (4.4) on phenomenological grounds and the chiral relation $F_2^A = F_2^V$, we can predict eq. (4.2).

It has to be noted however that our result is stricly correct only for the transverse contribution to $F_2^\gamma(\omega)$. A factor (1+R), with $R \equiv \sigma_L / \sigma_T$, should appear in (4.4). It follows therefore that the exact fulfillment of (4.4) implies R=0 as $\omega \to \infty$, in agree-

ment with the quark parton model, with only spin 1/2 constituents.

Let us consider now inelastic neutrino- and antineutrino-nucleon scattering. The main idea is to relate, in the framework of a simple Regge model, the structure functions for νN and $\bar{\nu} N$ scattering to those for eN scattering, explicitly given by eqs. (3.13) both for protons and neutrons. Most of our results hold more generally than in a simple Regge picture, and can be obtained applying general constraints of hadrons duality to the structure functions[5].

The t channel quantum numbers and the corresponding Regge trajectories for the structure functions are shown in Table I[42].

TABLE I

t channel quantum numbers for Regge contributions to the structure functions[42].

Structure Functions	$(-1)^J P$	$(-1)^J C$	I^G	Regge Trajectories
$F_{1,2}^{\gamma p} + F_{1,2}^{\gamma n}$	+	+	0^+	P, f, f'
$F_{1,2}^{\gamma p} - F_{1,2}^{\gamma n}$	+	+	1^-	A_2
$F_{1,2}^{\nu p} + F_{1,2}^{\nu n}$	+	+	0^+	P, f, f'
$F_{1,2}^{\nu p} - F_{1,2}^{\nu n}$	+	+	1^+	ϱ
$F_3^{\nu p} + F_3^{\nu n}$	+	+	0^-	ω, φ
$F_3^{\nu p} - F_3^{\nu n}$	+	+	1^-	A_2

Assuming SU(3) symmetry for the factorized residues with the additional constraints of the quark model, and the equality of the vector and axial vector couplings we can express all the structure functions as follows (we neglect strangeness changing interactions, i.e. $\sin^2\theta_c \simeq 0$):

$$F_2^{\gamma p} + F_2^{\gamma n} = 2(a_p^V + a_p^S) + 2(a_{p'}^V + a_{p'}^S)\,\omega^{-1/2}, \tag{4.5a}$$

$$F_2^{\gamma p} - F_2^{\gamma n} = 2\,a_{A_2}\,\omega^{-1/2}, \tag{4.5b}$$

$$F_2^{\nu p} + F_2^{\nu n} = 8\,a_p^V + 8\,a_{p'}^V\,\omega^{-1/2}, \tag{4.5c}$$

$$F_2^{\nu n} - F_2^{\nu p} = 12\,a_{A_2}\,\omega^{-1/2}, \tag{4.5d}$$

$$F_3^{\nu p} + F_3^{\nu n} = -36\, a_{A_2}\, \omega^{1/2}, \tag{4.5e}$$

$$F_3^{\nu p} - F_3^{\nu n} = 12\, a_{A_2}\, \omega^{1/2}. \tag{4.5f}$$

Here a_i^V and a_i^S refer to the couplings of isovector and isoscalar photons respectively, $\alpha_p(0) = 1$ and $\alpha_i(0) = 1/2$ for all other trajectories. We have decoupled the nucleons from the pure strange φ and f' trajectories and assumed pure F couplings of the vector and tensor trajectories at the nucleon vertex. The D/F ratio obtained from analysis of hadronic reaction data is ~ -0.2, although it may be nearer to zero for V exchange than for T exchange[43]. Similar arguments give $a^V_{P'}/a_{A_2} = 5$ which agrees, through eqs. (4.5a-b), (3.6) and (3.7), with total photoproduction data on protons and neutrons.

Finally, using the fact that $a_i^S \simeq 2/9\, a_i^V$, we are left with only two unknowns a_P^V and $a_{P'}^V$ which are determined through eqs. (3.13):

$$\begin{aligned} a_P^V &\equiv F_2^V(\infty) = \frac{f_\pi^2}{\pi}\, \sigma_{\pi N}(\infty), \\ a_{P'}^V &= \frac{5 f_\pi^2 \sqrt{2M_p}}{12 m_\varrho}\, \beta_{\pi p}, \end{aligned} \tag{4.6}$$

where $\sigma_{\pi p}(\nu) \equiv \sigma_{\pi p}(\infty) + \beta_{\pi p}/\sqrt{\nu}$. The whole set of structure functions for both weak and electromagnetic inelastic processes in therefore determined and predicted from the knowledge of πp total cross sections or, equivalently, from photoproduction data.

Furthermore, from eqs. (4.5) we can derive a large set of relations among different structure functions which, although strictly true in the Regge region, are expected to hold, by duality, also in the small ω region. They also reproduce the results derived in the framework of the quark parton model[3]. Explicitly, from eqs. (4.5a) and (4.5c) we have:

$$F_2^{\nu N} \equiv \frac{1}{2}(F_2^{\nu p} + F_2^{\nu n}) = \frac{1}{2}(F_2^{\nu N} + F_2^{\bar\nu N}) = \frac{18}{5.5}\, \frac{1}{2}(F_2^{\gamma p} + F_2^{\gamma n}), \tag{4.7}$$

where the factor 5.5 in the denominator of the r.h.s. becomes 5 if we neglect the φ contribution to a_i^S in eq. (4.5a) ($a_i^S = \frac{1}{9} a_i^V$).

From eqs. (4.5b) and (4.5c) we have[44]

$$F_2^{\nu n} - F_2^{\nu p} = 6(F_2^{\gamma p} - F_2^{\gamma n}), \tag{4.8}$$

which allows one to derive the Gottfried sum rule[45] from the Adler sum rule[46].

From eqs. (4.5b) and (4.5f) we get the Llewellyn-Smith relation[47]

$$F_3^{\nu p} - F_3^{\nu n} = 6\omega (F_2^{\gamma p} - F_2^{\gamma n}) = 12 (F_1^{\gamma p} - F_1^{\gamma n}), \tag{4.9}$$

where the last equality assumes R=0.

From eqs. (4.5b), (4.5d) and (4.5a) we have:

$$\frac{F_3^{\nu p} + F_3^{\nu n}}{\omega} = -3 (F_2^{\nu n} - F_2^{\nu p}) = -18 (F_2^{\gamma p} - F_2^{\gamma n}), \tag{4.10}$$

which again relates the Gross-Llewellyn-Smith[48] sum rule to the Adler sum rule.

We can test these relations locally by comparison with the electron and neutrino data. The ratio of total neutrino and antineutrino cross sections is given by :

$$\frac{\sigma_{TOT}^{\bar{\nu} N}}{\sigma_{TOT}^{\nu N}} = \frac{2-B}{2+B} \quad , \tag{4.11}$$

with

$$B \equiv - \int_0^1 dx\, x F_3(x) \Big/ \int_0^1 dx\, F_2(x). \tag{4.12}$$

Using eqs. (4.7) and (4.10) we get:

$$B = 5.5 \frac{\int dx (F_2^{\gamma p} - F_2^{\gamma n})}{\int dx (F_2^{\gamma p} + F_2^{\gamma n})} \simeq 5.5 \frac{(0.16-0.12)}{(0.16+0.12)}^{49)} = 0.85, \tag{4.13}$$

to be compared with $B_{exp} = 0.90 \pm 0.04$[50] and B=1 in the quark parton model with purely fermion partons.

Similarly, from (4.7), we get for the total cross section summed over neutrino and antineutrino beams:

$$\sigma_{TOT}^{\nu N}(E) + \sigma_{TOT}^{\bar{\nu} N}(E) = \frac{G^2 M_N E}{\pi} \frac{4}{3} \left[\frac{1}{2} \int_0^1 dx (F_2^{\nu N} + F_2^{\bar{\nu} N}) \right] \cong \frac{G^2 M_N E}{\pi} \frac{4}{3} \left[0.46 \right],$$

to be compared with the experimental value (0.47 ± 0.07)[50].

It follows therefore that, within the present accuracy, the data support the approximate validity of the above relations also in the low ω region, where the integrals are experimentally evaluated.

To conclude, we have been able to reproduce all the results of the quark parton model without invoking point constituents but rather accomodating scaling in a fairly natural way by imposing on the current induced processes the regularities one observes in purely hadronic reactions. Furthermore, we have found consistent links among different processes as e^+e^- annihilation, photoproduction of vector mesons and total photoproduction on nucleons, πN scattering and deep inelastic electron and neutrino

scattering, in agreement with experiments.

5. INCLUSIVE DEEP INELASTIC PROCESSES.

In the previous sections we have discussed a picture of electromagnetic interactions which in addition to giving consistent relations between different processes at low values of q^2, provides also a nice description of scaling for q^2 large, both positive and negative. If, however, in e^+e^- annihilation scaling is essentially built up from the electromagnetic properties of the hadronic constituents of the photon, in deep inelastic scattering on the contrary we need in addition that the strong interactions themselves have to share the same scaling properties. This feature is also found in the production of massive lepton pairs in hadronic collisions, which has been analysed[7, 51] along the same lines.

In spite of the different physical interpretation of these deep inelastic phenomena, all our scaling results coincide with those of the parton model as far as the integrated cross sections are concerned. The mean departure from the parton model results concerns the Q^2 dependence of the inclusive distributions. In fact, as a result of the scaling assumptions for strong interactions, one finds for the inclusive distributions a super-scaled form depending only on dimensionless quantities,

$$\frac{1}{\sigma}\,\frac{d\sigma}{d^3k/k_o} \sim \left(\frac{1}{Q^2}\right) F\left(\omega_j,\, x_F,\, \frac{k_T^2}{Q^2}\right), \tag{5.1}$$

where ω_j are Bjorken variables, x_F is the Feynman variable and k_T can be either the transverse momentum of a massive photon ($q^2=Q^2$) produced in hadronic collisions, or the transverse momentum of a produced hadron stronghly correlated to a large q^2 photon, for example in the photon fragmentation region for deep inelastic scattering. Eq. (5.1) leads to a very strong prediction,

$$\langle k_T^2 \rangle \sim Q^2, \tag{5.2}$$

which has also been shown by Bjorken[52] to follow in models of this type from correspondence arguments.

In particular the idea that the average transverse size of virtual photons of mass Q^2 may decrease as $1/\sqrt{Q^2}$ has emerged from Cheng and Wu's[53] calculations in Q.E.D. A growth with Q^2 of the average transverse momentum of produced hadrons correlated to a virtual photon, has been also investigated by Abarbanel and Kogut[54] in the framework of multiperipheral models. Similar results have been obtained by Gonzales and Weis[55] in the framework of dual resonance models. Simple kinematical analysis generally shows that in the appropriate regions one is naturally led to $q_T^2 \sim Q^2$, unless and ad hoc cut-off in q_T itself is assumed, as in the parton model.

By using this concept of an average transverse momentum increasing with Q^2, we give a number of specific predictions concerning some inclusive processes like massive photon production, single particle electroproduction, and pure hadronic production at large transverse momenta, which can be easily tested, providing equally crucial tests for the parton model.

5.1. Lepton pairs production in hadronic collisions.

The production of massive lepton pairs in hadronic collisions has been extensively studied in Refs. 7 and 51. We briefly discuss here the main results.

Consider the deep inelastic process

$$\text{proton}(p_1) + \text{proton}(p_2) \to \gamma(q) + X \tag{5.3}$$

where $p_i^2 = m^2$, $q^2 = Q^2$ and X denote a system of hadrons. The kinematic variables are $s=(p_1+p_2)^2$; $t=(p_1-q)^2$; $u=(p_2-q)^2$, $M_X^2=(p_1+p_2-q)^2$, along with Bjorken and Feynman scaling variables

$$\begin{aligned} x_j^B &= 2(p_j q)/Q^2, \qquad j = 1, 2 \\ x_F &= 2 q_{/\!/}^{*} / \sqrt{s} = \frac{Q^2}{s} \; \frac{x_1^B - x_2^B}{\sqrt{1-4m^2/s}}, \end{aligned} \tag{5.4}$$

and a transverse scaling variable

$$x_T \equiv \frac{q_T^2}{Q^2} \quad \underset{x_j^B \text{ fixed}}{Q^2, s \text{ large}} \quad \frac{Q^2}{s}\,(x_1^B x_2^B - \frac{s}{Q^2}), \tag{5.5}$$

The single particle distribution function is defined as usual

$$f_{pp}^{\gamma}(q,s) \equiv \frac{1}{\sigma_{pp}^{tot}(s)} \; \frac{d\sigma^{\gamma}}{d^3q/q_o}. \tag{5.6}$$

The large Q^2 behaviour of f_{pp}^{γ} is related to the average transverse momentum dependence on Q^2. From eq. (5.5) it follows that in the Bjorken limit, s and Q^2 large with $\tau \equiv Q^2/s$ fixed, q_T^2 grows as Q^2 unless an ad hoc cut-off in q_T is assumed. In the parton model[56] this is exhibited in the form of a δ function in $(x_1^B x_2^B - 1/\tau)$.

To specify the form of f_{pp}^{γ}, we use the model developed above which visualizes the process as the strong production of an infinite number of vector mesons which then decay into $l\bar{l}$ pairs. With obvious notations we have:

$$\frac{d\sigma^{l\bar{l}}}{dQ^2} = \frac{\alpha^2}{3\pi}\left(1+\frac{2\mu^2}{Q^2}\right)\left(1-\frac{4\mu^2}{Q^2}\right)^{1/2} \frac{1}{Q^2} \sum_n \frac{4\pi}{f_n^2} \; \frac{m_n^4}{(m_n^2-Q^2)^2+m_n^2\Gamma_n^2} \; d\sigma_n(m_n^2, s), \tag{5.7}$$

where μ is the lepton mass and $d\sigma_n(m_n^2, s)$ refers to the inclusive cross-sections to produce a vector meson of mass m_n at the total center of mass energy squared s. (For semplicity the momentum variables are not shown).

Our scaling results for e^+e^- annihilation lead to the scaling behaviour of $d\sigma^{l\bar{l}}/dQ^2$ once a similar scaling behaviour is also shared by the strong cross sections σ_n, ($\sigma_n(m_n^2, s) \sim A F(m_n^2, s)/m_n^2$), similarly to what obtained in photo-and electroproduction. Furthermore, the full dependence of the dilepton distribution function on the different kinematical variables is essentially the same in our approach, as that of the hadronic inclusive distribution of mass Q^2 at c.m. energy $\sqrt{s}$. For example, for Q^2 large, but s/Q^2, t/Q^2, u/Q^2 also large we are in the so-called pionization region. Let us for simplicity restrict ourselves to this region only; the neglect of both fragmentation regions is of course not valid near the kinematical boundaries. Using a Regge-Muller analysis with only the leading (double) pomeron exchanges, and scaling both "photon"--proton subenergies as $(s_j/Q^2)^{\alpha_P}$, $j = 1, 2$, with constant residue functions, one finally gets

$$\frac{d\sigma^{l\bar{l}}}{dQ^2 dx_F dx_T} \simeq \frac{4\pi\alpha}{3Q^4}\left(1+\frac{2\mu^2}{Q^2}\right)\left(1-\frac{4\mu^2}{Q^2}\right)^{1/2} \frac{2A}{3\gamma f_\varrho^2} \frac{e^{-c_1 x_F^2} e^{-c_2 x_T^2}}{\sqrt{x_F^2+4Q^2(1+x_T)/s}}, \tag{5.8}$$

where $\gamma = \Gamma_n/m_n \simeq \Gamma_\varrho/m_\varrho$. In obtaining (5.8) we have explicitly summed up the series in (5.7) using our results of sect. 2.1 and assumed for the n-vector production in the central region the simple form

$$\frac{d\sigma_n}{dx_F\, dq_T^2} \sim \frac{A}{m_n^4} \frac{e^{-c_1 x_F^2} e^{-c_2 q_T^2/m_n^2}}{\sqrt{x_F^2+4(m_n^2+q_T^2)/s}}. \tag{5.9}$$

Both eqs. (5.8) and (5.9) manifestly reflect the increase of the average transverse momentum of the photon (vector meson) with $Q^2(m_n^2)$.

Eq. (5.8) with A, c_1 and c_2 as free parameters, is compared in the Figures 7-10, with the data from the BNL-Columbia experiment[57], which measured muon pairs in collision of protons with a uranium target at incident lab. energies from 22 to 29.5 GeV. The most salient features of this experiment are:

i) the production cross section varies smoothly with mass as $d\sigma/dQ \sim 1/Q^5$ for $1 \leq Q \leq$ ≤ 6 GeV;

ii) the total (integrated) cross section increases with energy by a factor of five over the range explored.

As clear from the Figures 7-10, both the above features are reproduced by (5.8). In particular the $1/Q^5$ behaviour of $d\sigma/dQ$, in agreement with the data, is obtained as follows: $1/Q^3$ comes from the scaling part, an extra $1/Q^2$ from the assumed

x_T cut-off and the experimental restriction to very small production angles. The sharp increase with energy of the observed total cross-sections arises experimentally due to the constraint on the pair lab. momentum ($q_L \gtrsim (q_L)_{min} = 12$ GeV/c), and theoretically due to the hadron-like behaviour of x_F distribution of the massive γ production ($\langle x_F \rangle$ changes at each incident proton energy). All the other features of the data are also satisfactories reproduced, in spite of our simple approximation (5.9) over the entire kinematical region explored.

The fitted values of the free parameters, $c_1 \simeq 8$, strikingly close to the π x-distributions, and $c_2 \simeq 2.3$ can be used now to consistently predict through (5.9), the vector meson inclusive distributions. The inclusive ϱ-meson cross section in pp collision has been very recently measured[58] at 12 GeV/c and 24 GeV/c and the observed features agree indeed quite well with our predictions. The p_T^2 distributions infact show an exponential falloff with a slope 3.6 ± 0.4 GeV^2 at both energies, to be compared with our $c_2/m_\varrho^2 \simeq 3.8$. The y distributions show that ϱ's come predominantly from the central region, thus we can also compare the s dependence of the measured cross sections with (5.9). We easily find $\sigma_1(24\ \text{GeV/c})/\sigma_2(12\ \text{GeV/c})\ \ln(s_1/2c_1 m_\varrho^2)/\ln(s_2/2c_1 m_\varrho^2) \simeq 1.7$ to be compared with $(3.50 \pm 0.42\ \text{nb})/(1.80 \pm 0.25\ \text{mb}) \approx 1.9$. With the fitted normalization in (5.8) we also obtains, within a factor $2 \div 3$, the absolute ϱ cross sections.

The overall picture is therefore selfconsistent and in very good agreement with experiments. Large mass photons are predicted to be produced with typical hadron-like features and a rate $(d\sigma/dQ)_\gamma \sim \alpha^2 (d\sigma/dm)_{had}$. From the lack of an absolute transverse momentum cut-off, which is the stongest prediction of this approach (see Fig. 11 for a typical distribution expected at ISR energies) a similar behaviour is expected to hold at large angles. This is in agreement with the preliminary observations of single leptons inclusively produced at 90°[59]. This results have to be contrasted with those of the parton model[56], where the angular distribution of lepton pairs is expected to be highly peaked in the beam direction. Furthermore this model is also strongly constrained from the bounds[60] on the antiquark content of the proton derived using electro-and neutrino-production experiments. These (upper) bounds an very much smaller than the experimental yields.

5.2. Inclusive electroproduction[8]

We would like to discuss now the implications of our picture for inclusive electroproduction with particular emphasis on the Q^2 dependence of the single particle distribution functions which, in the photon fragmentation region, turn out to be similar to that found above. Let us define

$$f(s, q^2, k_L, k_T) \equiv \frac{1}{\sigma_{tot}(s, q^2)} \frac{d\sigma}{d^3k/k_o} \qquad (5.10)$$

where k_L and k_T denote the longitudinal and transverse momenta of the detected hadron. In our picture of a hadron-like photon we can apply a Mueller-Regge analysis of the process, similarly to what we have done in the production of a massive photon. Both in the nucleon fragmentation region and in the central region, by virtue of the factorization of Regge residues, one obtains for f results similar to any other hadronic process, photoproduction being of course the most natural process to compare with. In going to the photon fragmentation region (s, q^2 large with ω fixed, and $x=k_L/k_{L_{max}}>0$), we find new, we find new, interesting, and quite different results concerning the q^2 dependence of f, essentially due to the increase of $\langle k_T^2 \rangle$ with q^2 x).

In the laboratory frame, denoting by z the longitudinal fraction of the momentum taken by k, i.e., $k_L = z\nu$, mere kinematics tells us that $k_T^2 \simeq q^2 z(z+2(qk)/q^2)$ for $\nu^2 \gg q^2$. Therefore, unless an a priori q^2 independent cut-off in k_T is assumed, we are naturally led to $\langle k_T^2 \rangle \sim q^2$, as in the processes previously discussed. This implies

$$f(s, q^2, k_L, k_T) \underset{\omega, x, x_T \text{ fixed}}{\overset{s, q^2 \to \infty}{\sim}} \frac{1}{q^2} G(\omega, x, x_T), \tag{5.11}$$

where we have defined $x_T = k_T^2/q^2$. Using Mueller-Regge arguments we finally obtain:

$$\sigma_{tot}(\nu, q^2) f(\nu, q^2, k_L, k_T) \underset{\omega, x, x_T \text{ fixed}}{\overset{\nu, q^2 \to \infty}{\longrightarrow}} \frac{1}{\nu} \frac{1}{q^2} \sum_i \omega^{\alpha_i} \beta_i(x, x_T), \tag{5.12}$$

where the sum is extended to both Pomeron and ordinary Regge trajectories and the functions β_i are damped in x_T. The extra factor $1/q^2$ in (5.12) has to be compared with the analogous factor present in eq. (5.8). From the general form of (5.12) one can deduce the following general features:

i) the transverse momentum distributions in the γ fragmentation region should broaden with increasing q^2. This q^2 variation would not manifest itself in the proton fragmentation nor central regions.

ii) For $k_T \approx 0$ the longitudinal momentum distributions will decrease with increasing q^2. Again this drop will not be present in the other two regions.

iii) The extra q^2 dependence in the denominator of the right-hand side of (5.12) will lead to a faster decrease of the diffractive contributions with respect to the contributions coming from the non-leading Regge trajectories. This will favour therefore the I = 1 exchanges with the proton, leading to asymmetries in the particle-antiparticle yields. In this sense the photon does "discriminate" between the charges. The composition of the observed final states will consequently also be affected.

---

x) See also Refs. (55) and (61).

All these characteristics are present in the main features of the present data[62]. It will be of course interesting to see if the actual trend continues to higher energies and large q^2. It should be again emphasized that the observation of the increase of the average transverse momentum with q^2, together with the associated effects we have just discussed, provides also a crucial test for the parton model.

5.3. Hadronic production at large $p_\perp$[51]

Since our previous arguments in section 5.1 were based on the hadronic cross-sections scaling in a specific way, it is natural to ask for some other conseqeunces of such a hypothesis. Indeed, due to the lack of an absolute transverse momentum cut-off, we would expect an abundant hadronic production at large angles with a rate of the order of $(d\sigma/dm)_{had} \sim 1/\alpha^2 (d\sigma/dm)_{em}$.

Recent ISR and NAL experiments[63] have shown rather large cross-sections at high $p_\perp$. Theoretically, this had led to proposals[64] which try to obtain slowly decreasing distributions (with $p_\perp$) with a parton-like view of the strong interactions. In our model, such a behaviour arises due to the above mentioned scaling properties.

The physical picture is very simple. In high energy hadronic collisions large masses can be produced with a law similar to (5.8), with no absolute cut-off in q_T, which subsequently decay into the particle finally detected with the transverse momentum p_T, plus everything else. By integrating on the intermediate momentum and mass spectrum one finds:

$$\left.\frac{d\sigma}{d^3p/p_0}\right|_{90^\circ} \underset{\text{large } p_\perp}{\sim} \left(\frac{1}{p_\perp}\right)^4 F\left(\frac{2p_\perp}{\sqrt{s}}\right) \qquad (5.13)$$

as guessed from dimensional analysis, where $F(2p_\perp/\sqrt{s})$ is a scaling function of the argument which depends on the threshold behaviour of the decay mechanism. Notice that the form (5.13) depends crucially on the existence of our x_T cut-off in the $q_\perp$ distribution function. The usual q_T cut-off will obtain a Gaussian but never a polynomial decrease with $p_\perp$. In our model, since the Q^2 integral is roughly dominated by masses of the order of $2p_\perp$, an immediate and observable consequence is the associated production of a bunch of particles in the opposite direction of $p_\perp$.

The generalization of eq. (5.13) to angles other than 90° can be expressed in the form $p_0 d\sigma/d^3p \sim (1/p_\perp)^4 F(x, p_\perp/\sqrt{s})$ where the function F saturates faster with increasing x, the asymptotic value sharply ($\sim$Gaussian) falling in x.

6. CONCLUSIONS

We have discussed a simple model of electromagnetic interactions which successfully describes the main features of high energy processes, involving real, space-like and time-like photons, relating different processes with a high degree of predictive po-

wer. The model has been successfully extended to neutrino deep inelastic phenomena, reproducing all the results of the quark parton model and providing further and consistent links among a wide class of different processes. The exhibited scaling properties, and the consequent point-like behaviour of the cross-sections, do not follow however from the existence of any elementary constituents, but rather from the sharing of similar scaling properties of strong and electromagnetic interactions. Although the results of scaling for the integrated cross-sections are the same as in the parton model, the absence of an absolute transverse momentum cut-off leads to quite different and easily testable predictions for the inclusive distributions.

Particular emphasys has been put to make clear the relations among the different reactions and how the various assumptions fit together and contrast one another. Experimental tests have also been indicated, where necessary, to verify the validity of this unconventional approach to deep inelastic phenomena. Further experiments will therefore be of great relevance to this concern, as well as providing crucial tests for the parton model.

It is pleasure to thank Y. Srivastava for his comments and a critical reading of the manuscript. The author is also grateful to his colleagues at Frascati for many valuable discussions.

* * * *

REFERENCES

1) R. P. Feynman, Phys. Rev. Letters 23, 1415 (1969).

2) J. D. Bjorken and E. A. Paschos, Phys. Rev. 185, 1975 (1969).

3) For a review see for example C. H. Llewellyn-Smith, Phys. Reports 3C, 261 (1972); F. J. Gilman, lectures at the Summer Institute on Particle International at Very High Energies, Louvain, Belgium (1973); SLAC-PUB-1338 (1973).

4) G. Tarnopolsky, J. Eshelman, M. E. Law, L. Leong, H. Newman, R. Little, K. Stranch and R. Wilson, Phys. Rev. Letters 32, 432 (1974); B. Richter, Proc. of Trieste Conf. on Colliding Beam Interactions, IAEA, Trieste (1974).

5) See for example M. Chaichian, S. Kitakado, S. Pallua, B. Renner and J. De Azcarraga, Nuclear Phys. 51B, 221 (1973).

6) A. Bramon, E. Etim and M. Greco, Phys. Letters 41B, 609 (1972).

7) E. Etim, M. Greco and Y. Srivastava, Phys. Letters 41B, 507 (1972).

8) M. Greco, Nuclear Phys. 63B, 398 (1973).

9) J. J. Sakurai and D. Schildknecht, Phys. Letters 40B, 121 (1972); 41B, 489 (1972); 42B, 216 (1972). See also J. J. Sakurai, lectures presented at the Intern. School of Subnuclear Phys., Erice, (1973).

10) M. Greco, Frascati preprint LNF-74/26(P) (1974), and Physics Letters, to be published.

11) G. Barbarino, F. Ceradini, M. Conversi, M. Grilli, E. Iarocci, M. Nigro, L. Paoluzi, R. Santonico, P. Spillantini, L. Trasatti, V. Valente, R. Visentin and G. T. Zorn, Lettere Nuovo Cimento 3, 689 (1972).

12) H. H. Bingham, W. B. Fretter, W. J. Podolsky, M. S. Rabin, A. H. Rosenfeld, A. Smadja, G. P. Yost, J. Ballam, G. B. Chadwick, P. Seyboth, I. O. Stillicorn, H. Spitzer and G. Wolf, Phys. Letters 41B, 635 (1972).

13) See for example G. Wolf, Proc. 1971 Intern. Conf. on Electron and Photon Interactions at High Energies, Ithaca, Cornell University (1972).

14) V. Alles Borelli, M. Bernardini, D. Bollini, P. L. Brunini, E. Fiorentino, T. Massam, L. Monari, F. Palmonari, F. Rimondi and A. Zichichi, Phys. Letters 40B, 433 (1972);

15) M. Conversi, L. Paoluzi, F. Ceradini, S. D'Angelo, M. L. Ferrer, R. Santonico, M. Grilli, P. Spillantini and V. Valente, Phys. Letters, to be published.

16) J. J. Sakurai, Phys. Letters 46B, 207 (1973); see also J. J. Sakurai, Erice lectures 1973, Ref. (9).

17) E. Etim and M. Greco, Frascati preprint LNF-74/31(P) (1974); E. Etim and M. Greco, to be published.

18) R. J. Crewther, Phys. Rev. Letters 28, 1421 (1972).

19) M. S. Chanowitz and J. Ellis, Phys. Letters 40B, 387 (1972); Phys. Rev. D7, 2490 (1970).

20) S. Weinberg, Phys. Rev. 118, 838 (1960); W. Zimmermann, Commun. Math. Phys. 11, 1 (1969); S. Coleman and R. Jackiw, Ann. Phys. 67, 552 (1971).

21) For a comparison among all the results on $e^+e^- \rightarrow$ hadrons at Adone, CEA and SPEAR, see for example G. Salvini, Erice lectures 1974.

22) M. Greco and Y. N. Srivastava, Frascati preprint LNF-74/52(P) (1974), and to be published.

23) M. Greco and Y. N. Srivastava, Nuovo Cimento 18A, 601 (1973).

24) E. Bloom and F. Gilman, Phys. Rev. Letters 25, 1140 (1970).

25) D. Schildkuecht, Erice Lectures 1974; see also H. Fraas, B. J. Read and D. Schildknecht, DESY preprint 74/23 (1974).

26) V. Rittenberg and H. R. Rubinstein, Nuclear Phys. B28, 184 (1971); see also H. D. I. Abarbanel, M. L. Goldberger and S. B. Treiman, Phys. Rev. Letters 22, 500 (1969).

27) Wu-Ki Tung, Phys. Rev. Letters 23, 1531 (1969).

28) V. Gribov, Fourth Winter Seminar on the Theory of the Nucleus and the Physics of High Energies, 1969, Ioffe Institute of Engineering Physics, Acad. Science USSR; J. D. Bjorken, Proc. of Summer Institute on Particle Physics (1973); SLAC Report n. 167, Volume I.

29) That includes deep inelastic scattering both with muons and neutrinos at large q^2. For the muon beam results see D. J. Fox et al., Contrib. n. 330 to the XVII Conf. on High Energy Physics, July 1974, London; For neutrino beam results see Ref. 50. For a recent review on scaling, see F. J. Gilman, Rapporteur's Talk to the London Conference, SLAC-PUB-1455 (1974).

30) J. Bell, Phys. Rev. Letters 13, 57 (1964); CERN Report TH-877; L. Stodolsky, Phys. Rev. Letters 18, 135 (1967).

31) D. O. Caldwell, V. B. Elings, W. P. Hesse, G. E. Jahn, R. J. Morrison, F. V. Murphy and D. E. Yount, Phys. Rev. Letters 23, 1256 (1969); W. L. Lakin, T. J. Braunstein, J. Cox, B. D. Dieterle, M. L. Perl, W. T. Toner, T. F. Zipf and H. C. Bryant, Phys. Rev. Letters 26, 34 (1971); V. Heynen, H. Meyer, B. Naroska and D. Notz, Phys.

Letters 34B, 651 (1971); See also K. Gottfried, 1971 Intern. Conf. on Electron and Photon Interactions at High Energies, Ithaca, Cornell University (1972); H. W. Kendall, ibid.

32) K. Gottfried and D. Yennie, Phys. Rev. 182, 1595 (1969); S. J. Brodsky and J. Pumplin, Phys. Rev. 182, 1794 (1969); B. Margolis and C. Tang, Nuclear Phys. B10, 329 (1969); M. Nauenberg, Phys. Rev. Letters 22, 556 (1969); B. Gribov, JETP 30, 709 (1970).

33) In addition to Refs. 30 and 32 see also D. R. Yennie, "Hadronic Interactions of Electrons and Photons" adited by J. Cumming and H. Osborn (Academic Press, 1971); K. Gottfried, Ref. 31; H. W. Kendall; ibid.

34) See K. Gottfried, Ref. 31; W. H. Kendall, ibid.

35) M. Greco and Y. N. Srivastava, Phys. Letters 51B, 172 (1974).

36) D. Schildknecht, Nuclear Phys. B66, 398 (1973).

37) See for example H. Joos, Hadronic Interactions of Electrons and Photons (edited by J. Cumming and H. Osborn) (Academic Press, 1971).

38) P. Langacker and M. Suzuki, Phys. Letters 40B, 561 (1972); Phys. Rev. D7, 273 (1973).

39) K. Fujikawa and P. J. O'Donnell, Phys. Rev. D8, 3200 (1973).

40) K. Kawarabayashi and M. Suzuki, Phys. Rev. Letters 16, 255 (1966); Fayazaddin and Riazuddin, Phys. Rev. 147, 1071 (1966).

41) H. Pagels, Rockefeller University preprint (1972) (unpublished).

42) H. Pagels, Phys. Rev. D3, 1217 (1971); see also C. H. Llewellyn-Smith, Ref. 3.

43) C. Michael, Springer Tracts in Modern Physics, (edited by G. Hohler), Vol. 55 (Springer, Berlin, 1970).

44) P. M. Fishbane and D. Z. Freedman, Phys. Rev. D5, 2582 (1972).

45) K. Gottfried, Phys. Rev. Letters 18, 1174 (1967).

46) S. L. Adler, Phys. Rev. 143, 144 (1966).

47) C. H. Llewellyn-Smith, Nuclear Phys. B17, 277 (1970).

48) D. J. Gross and C. H. Llewellyn-Smith, Nuclear Phys. B14, 337 (1969).

49) J. S. Poucher, M. Breidenbach, R. Ditzler, J. I. Friedman, H. W. Kendall, E. D. Bloom, R. L. A. Cottrell, D. H. Coward, H. De Staebler, C. L. Jordan, H. Piel and R. E. Taylor, Phys. Rev. Letters 32, 110 (1974).

50) P. Musset, Proc. II Intern. Conf. on Elementary Particles, Aix-en-Provence (1973), and references therein. See also F. J. Gilman, Ref. 3.

51) M. Greco and Y. N. Srivastava, Nuclear Phys. B64, 531 (1973).

52) J. D. Bjorken, Ref. 28.

53) H. Cheng and T. T. Wu, Phys. Rev. 183, 1324 (1969).

54) H. D. I. Abarbanel and J. B. Kogut, Phys. Rev. D5, 2050 (1972).

55) M. A. Gonzales and J. H. Weis, Phys. Letters 49B, 351 (1974).

56) S. D. Drell and T. M. Yan, Phys. Rev. Letters 25, 316 (1970); P. V. Landshoff and J. C. Polkinghorne, Nuclear Phys. B33, 221 (1971).

57) J. H. Christenson, A. S. Hicks, L. M. Lederman, P. J. Limon, B. J. Pope and E. Zavattini, Phys. Rev. Letters 25, 1523 (1970).

58) Bonn-Hamburg-Munich collaboration, contributed paper to the 1973 Aix-en-Provence

Conference on Elementary Particles; see also F. Winkelman, talk given at the IV Intern. Conf. on Experimental Meson Spectroscopy, Boston (1974).

59) V. Abramov et al., Contrib. n. 785 to the XVIII Intern. Conf. on High Energy Physics, London (1974); J. P. Appel et al., contrib. n. 571 and 1023, ibid.; D. Bintenger et al., contrib. n. 576, ibid., R. Birge et al., contrib. n. 1050, ibid.; J. P. Boymond et al., contrib. n. 398, ibid.; S. Segler et al., contrib. n. 218, ibid.

60) G. R. Farrar, Nuclear Phys. B77, 429 (1974); R. Savit and M. B. Einhorn, Phys. Rev. Letters 33, 392 (1974).

61) J. Cleymans, SLAC-PUB-1119 (1972), unpublished.

62) K. Berkelman, Invited talk given at the XVI Intern. Conf. on High Energy Physics, Batavia, (1972), 111.

63) For a review see M. Jacob, Erice Lectures (1974).

64) S. M. Berman, J. D. Bjorken and J. B. Kogut, Phys. Rev. D4, 3388 (1971); J. F. Gunion, S. J. Brodsky and R. Blankenbecler, Phys. Rev. D6, 2652 (1972); D8, 287 (1973); P. V. Landshoff and J. C. Polkinghorne, Phys. Rev. D8, 927 (1973); 4159 (1973); D. Amati, L. Caneschi and M. Testa, Phys. Letters 43B, 186 (1973).

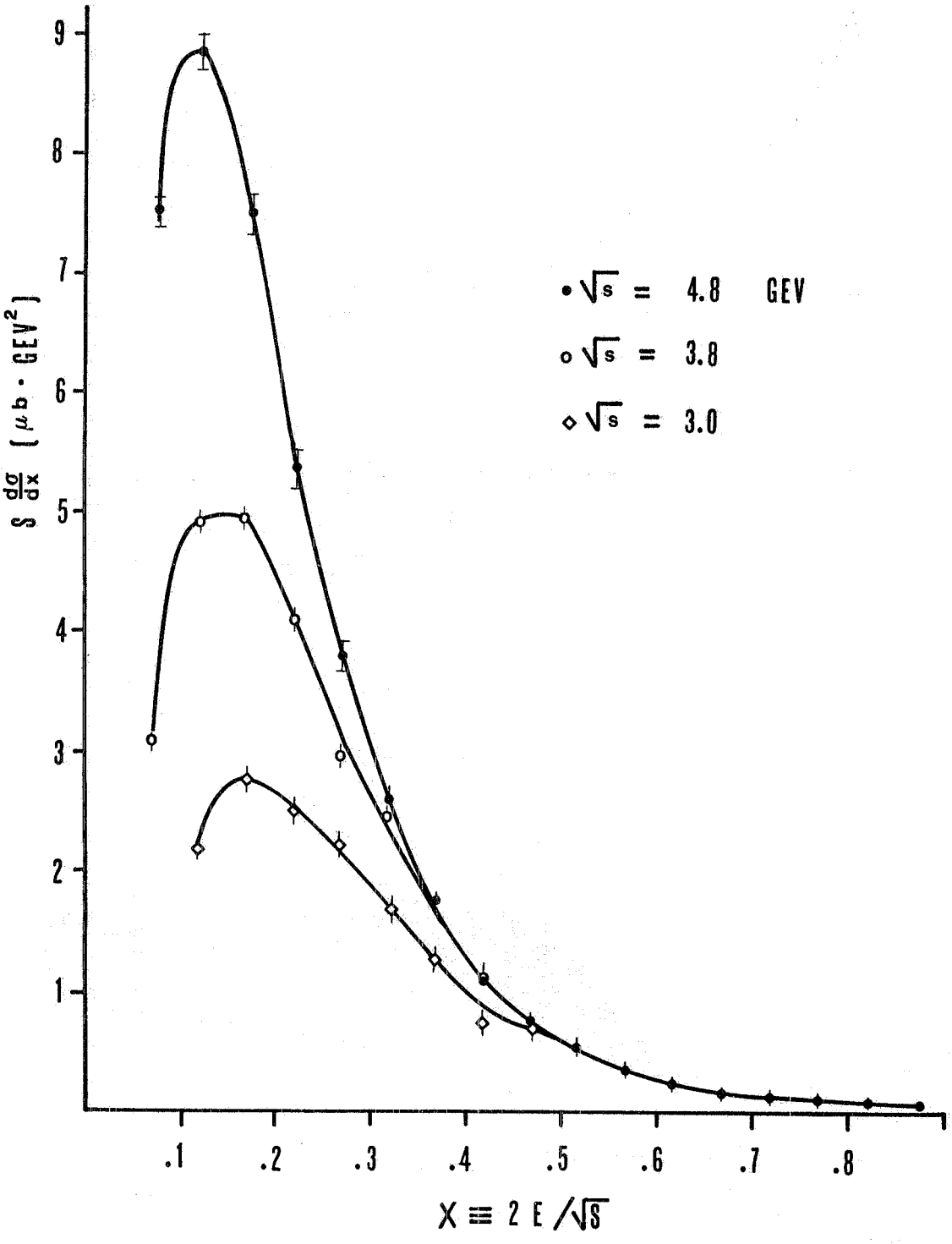

FIG. 1. Single inclusive pion distributions in e^+e^- annihilation as a function of x. The data are taken from Richter's talk at the Trieste Conf., Ref. 4.

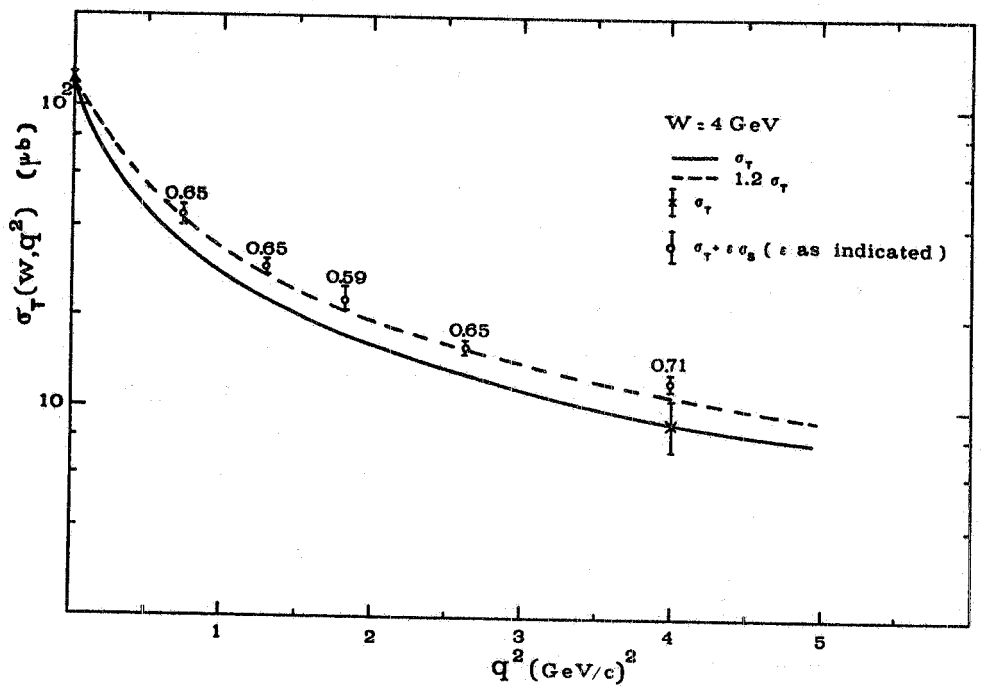

FIG. 2 Total transverse cross section $\sigma_T(\nu, q^2)$ for fixed $W \equiv \sqrt{s}$.

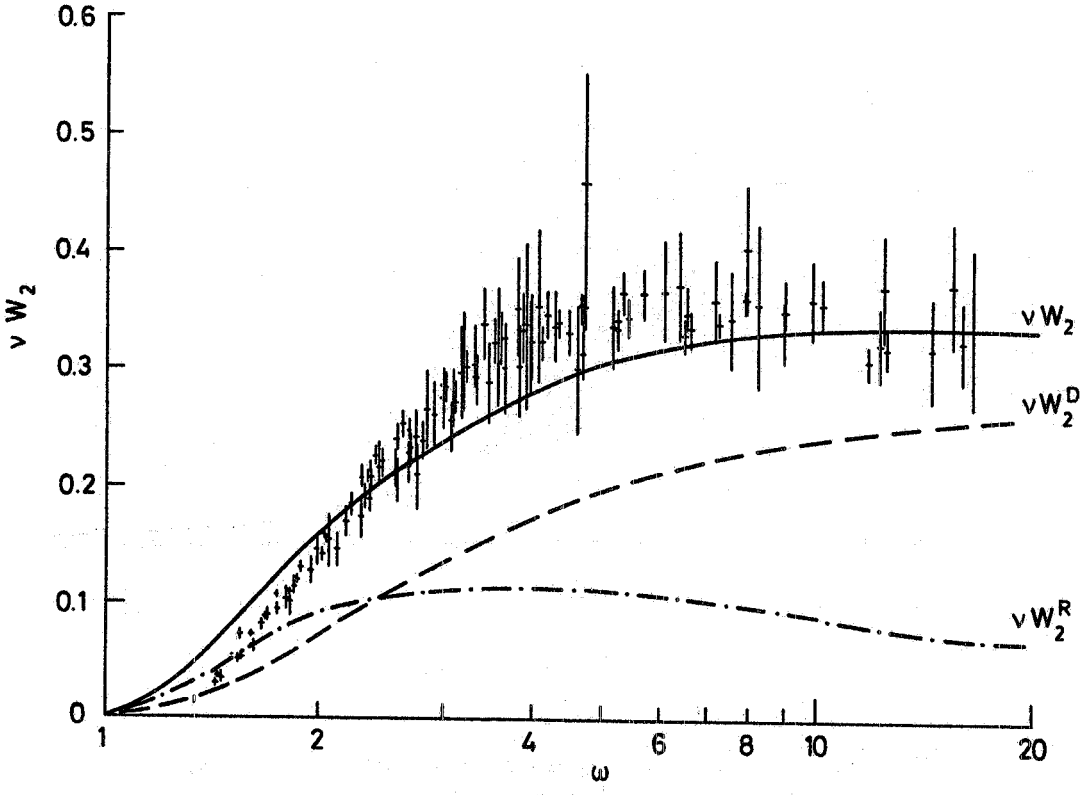

FIG. 3 Diffractive (D) and resonant (R) contributions to the sturcture function νW_2.

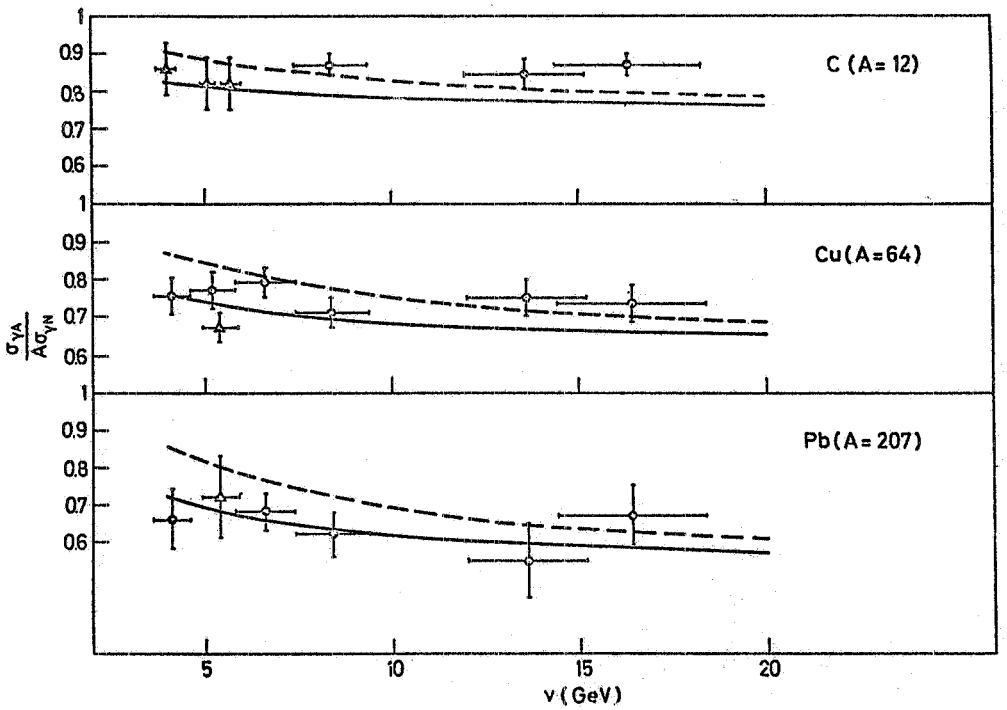

FIG. 4 Predictions for $\sigma_{\gamma A}(\nu)/A\,\sigma_{\gamma N}(\nu)$ in photoproduction for various nuclei. The dashed line corresponds to $\eta = 0$, the full line to $\eta = \eta_{\text{Compton}}$. η is defined as the ratio of the real to imaginary part of the vector-nucleon forward scattering amplitude. The data are taken from Ref. 31.

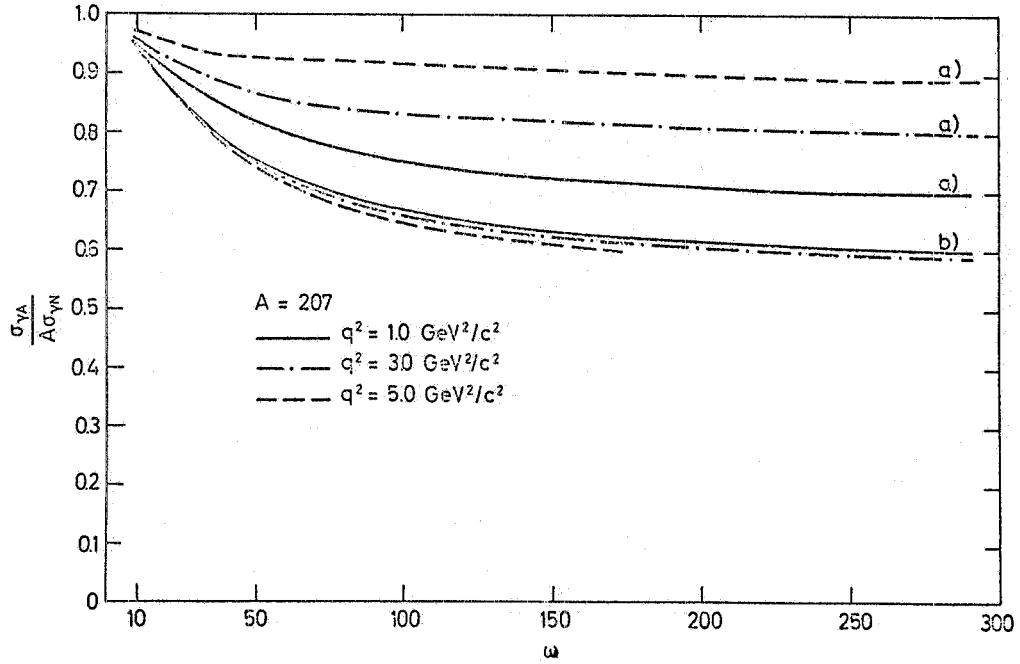

FIG. 5 Predictions for $\sigma_{\gamma A}(\nu, q^2)/A\,\sigma_{\gamma N}(\nu, q^2)$ as a function of $\omega = 2M\nu/q^2$ and q^2. The curves a) and b) refer to the case $\sigma_n \sim 1/m_n^2$ (our approach) and $\sigma_n \sim$ const (Schildknecht, Ref. 36) respectively.

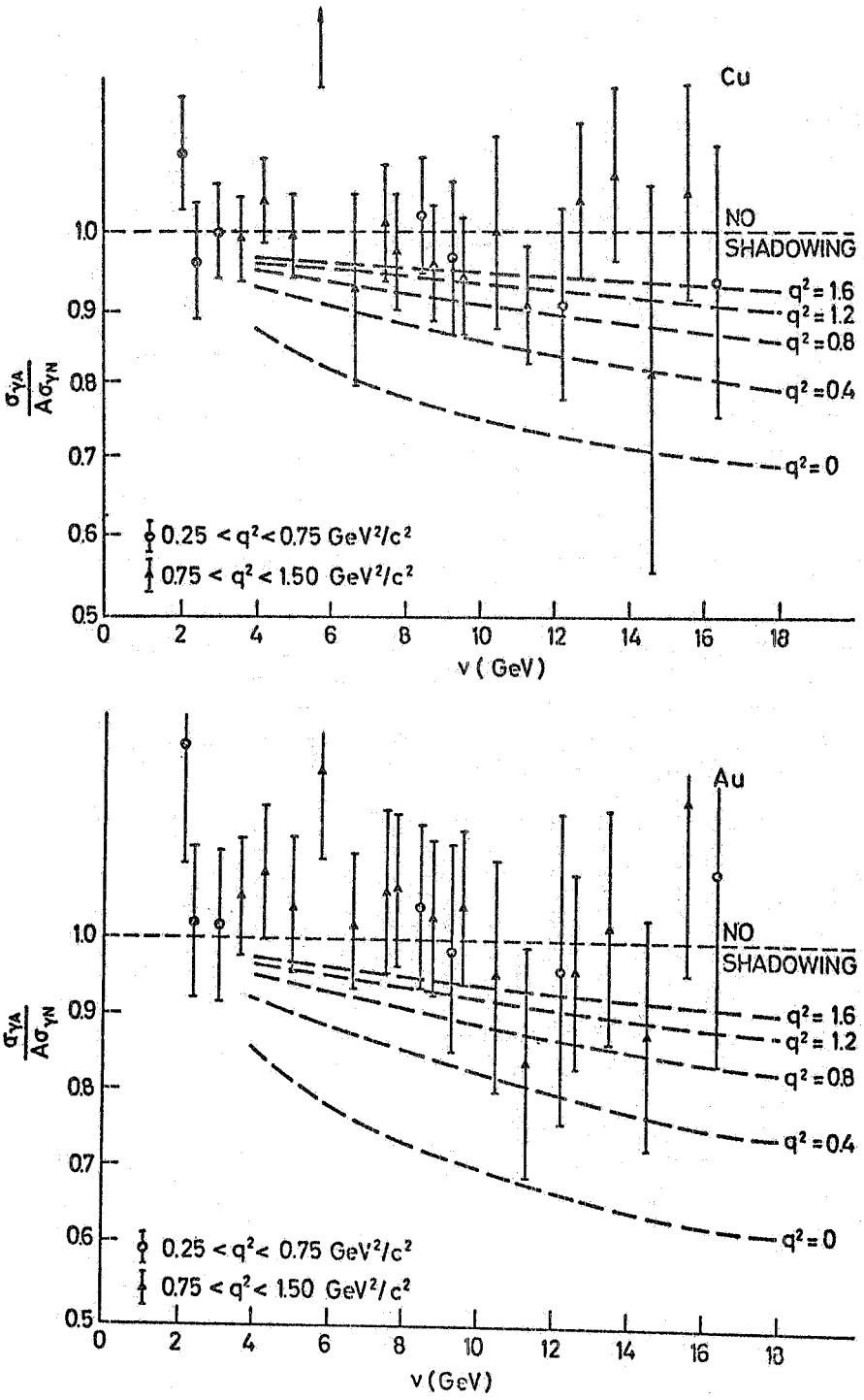

FIG. 6 Predictions for $\sigma_{\gamma A}(\nu, q^2)/A\ \sigma_{\gamma N}(\nu, q^2)$ as a function of the photon energy ν and photon mass squared $-q^2$. The data are taken from Ref. 31.

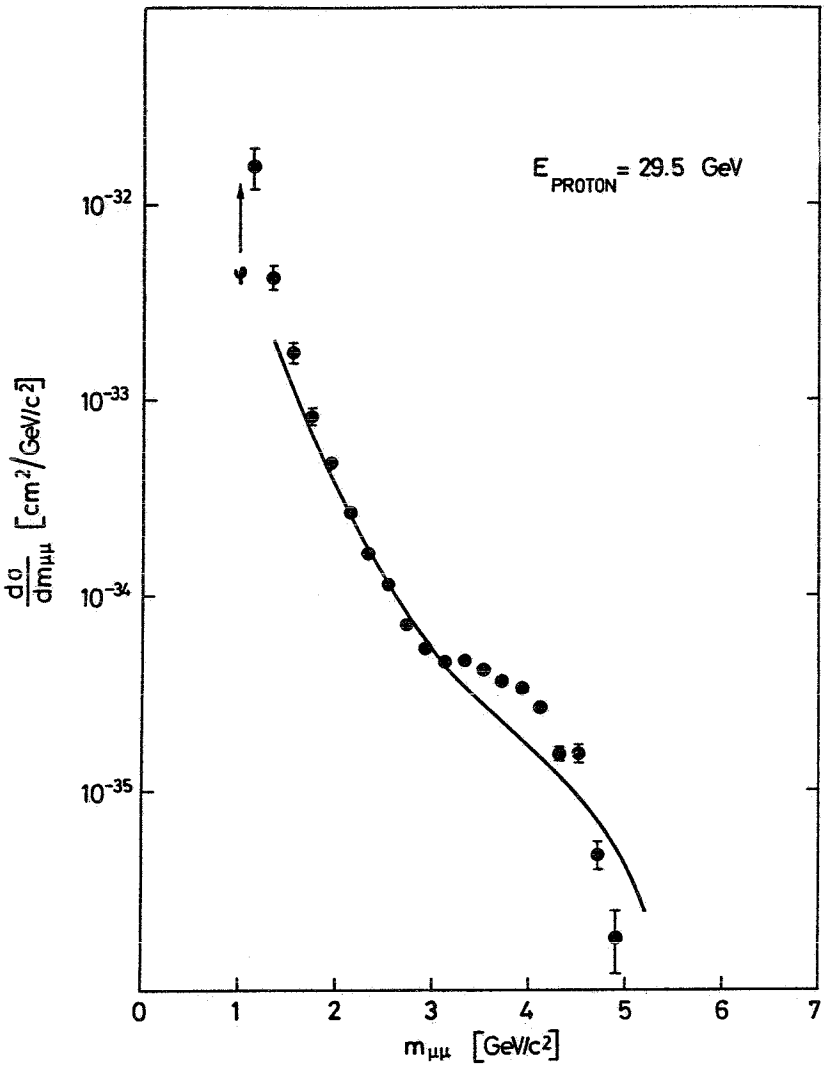

FIG. 7 $d\sigma/dm_{\mu\mu}$ as a function of the di-muon mass $m_{\mu\mu}$. The data refer to the experiment of Ref. 57.

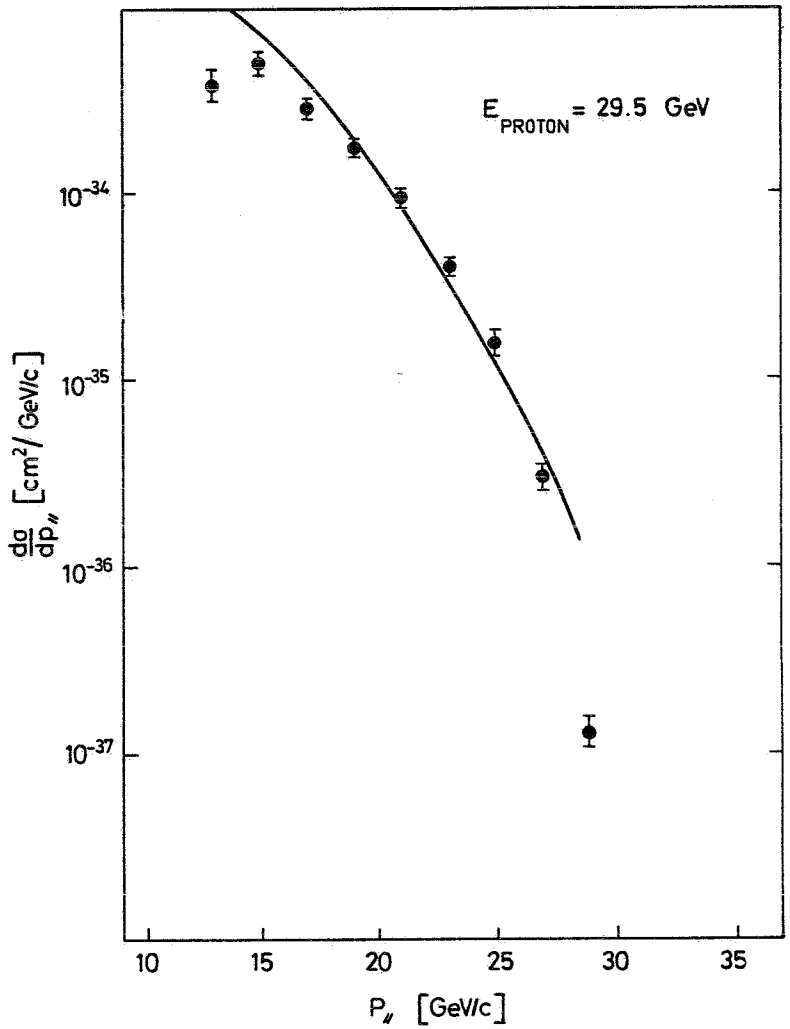

FIG. 8 $d\sigma/dp_{||}$ as a function of the longitudinal lab. di-muon momentum $p_{||}$. The data refer to the experiment of Ref. 57.

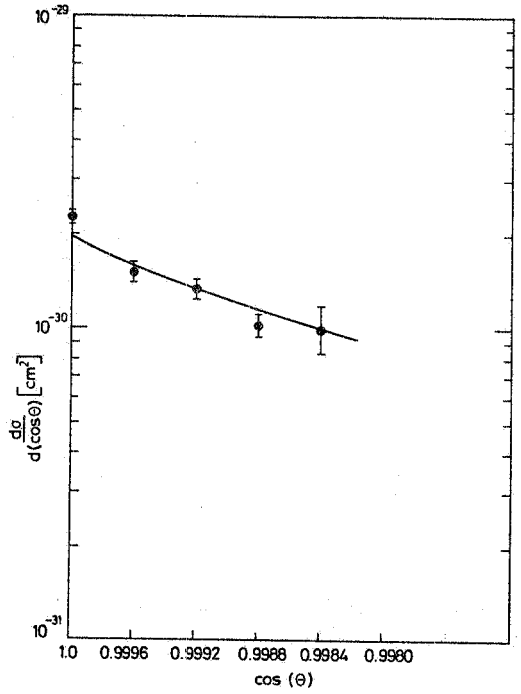

FIG. 9 $d\sigma/d(\cos\theta)$ as a function of $\cos\theta$, where θ is the production angle of the pair, with respect to the beam direction. The data refer to the experiment of Ref. 57.

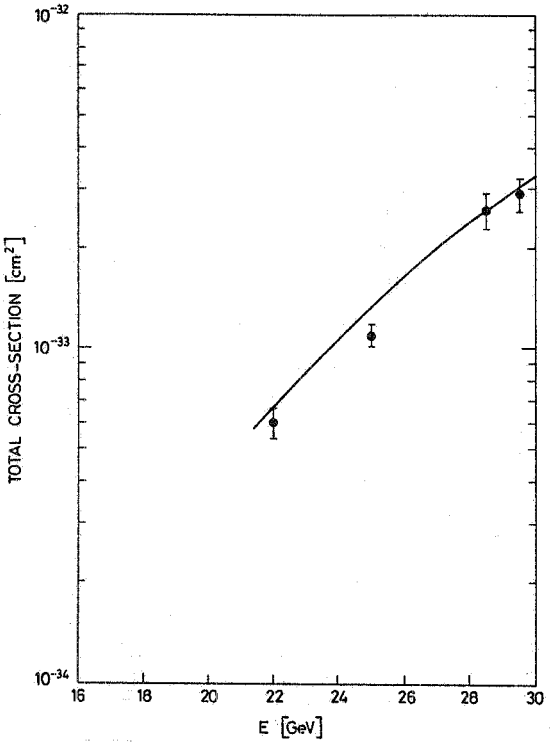

FIG. 10 Total cross section as a function of incident energy, in the experiment of Ref. 57.

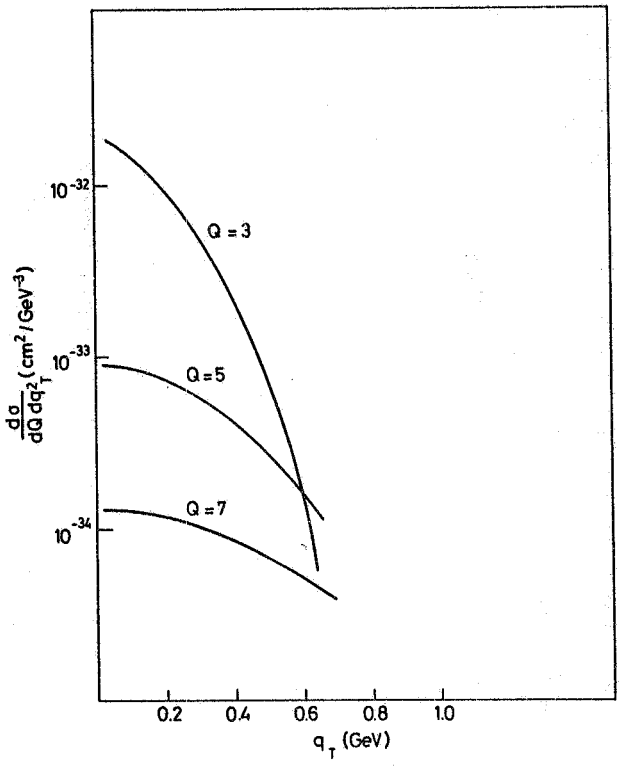

FIG. 11 Predictions for $d\sigma/dQdq_T^2$ as a function of q_T, for different values of Q, at $s = 950$ GeV^2.